TECHNO- ECONOMIC ANALYSIS OF WASTEWATER SLUDGE GASIFICATION: A DECENTRALIZED URBAN PERSPECTIVE

by

Nicholas P. G. Lumley

A thesis submitted to the Faculty and the Board of Trustees of the Colorado School of Mines in partial fulfillment of the requirements for the degree of Master of Science (Mechanical Engineering).

Golden, Colorado

Date _____

Signed: _____
Nicholas P. G. Lumley

Signed: _____
Dr. Jason Porter
Thesis Advisor

Golden, Colorado

Date _____

Signed: _____
Dr. Gregory Jackson
Professor and Head
Department of Engineering

ABSTRACT

Wastewater sludge management is a significant challenge for small-scale, urban wastewater treatment plants (WWTPs). Common management strategies stabilize sludge for land disposal by microbial action or heat. Such approaches require large footprint processing facilities or high energy costs. A new approach considers sludge to be a fuel which can be used on-site to produce electricity. Electrical power generation fueled by sludge may serve to reduce the volume of hazardous waste requiring land disposal and create economic value for WWTP operators. To date, no detailed system designs or techno-economic analyses have been found for small scale sludge fueled power plants. Fortunately, a literature base exists describing the fundamentals of applying thermochemical conversion (TCC) technologies to sewage sludge. Thermochemical conversion of sludge is established for large WWTPs, however large system design techniques may not be applicable to small systems.

To determine the feasibility of small scale power generation fueled by sludge, this work evaluates several thermochemical conversion technologies from the perspective of small urban WWTPs. Literature review suggests wet oxidation, direct combustion, pyrolysis, and gasification as candidate front-end TCC technologies for on-site generation. Air and steam blown gasification are found to be the only TCC technologies appropriate for sludge. Electrical power generation processes based on both air and steam blown gasification are designed around effective waste heat recovery for sludge drying. The systems are optimized and simulated for net electrical output in ASPEN Plus®. Air blown gasification is found to be superior. Sensitivity analyses are conducted to determine the effect of fuel chemical composition on net electrical output. A technical analysis follows which determines that such a system can be built using currently available technologies. Finally, an economic analysis concludes that a gasification based power system can be economically viable for WWTPs with raw sewage flows of 0.115 m^3/s, or about 2.2 million gallons per day.

TABLE OF CONTENTS

LIST OF FIGURES

LIST OF TABLES

LIST OF SYMBOLS

Carbon conversion efficiency . . . . . η_c

Chemical potential . . . . . μ

Cost C

Dewpoint temperature . . . . . T_{dewpoint}

Fraction of raw sludge converted to water . . . . . $Conv$

Electrical power in [kW] . . . . . kWe

Efficiency . . . . . η

Equilibrium constant . . . . . K

Equilibrium temperature . . . . . $T_{\text{equilibrium}}$

Equivalence ratio . . . . . ER

Experimental data . . . . . e

Electrial power . . . . . $\dot{W}_e$

Fraction of syngas diverted to burner . . . . . δ

General summation index i

Gibbs free energy of a mixture . . . . . G

Heat duty . . . . . $\dot{Q}$

Heat transfer from burner to gasifier . . . . . $\dot{Q}_{\text{burner}}$

Inflation rate . . . . . d

Mass flow . . . . . $\dot{m}$

Mass fraction . . . . . m

Mass specific enthalpy change of vaporization . . . . . Δh_{fg}

Model data . . . . . m

Molar flow rate . . . . . $\dot{y}$

Mole Fraction . . . . . χ

Net annual cash flow . . . . . F_n

Number of points in a summation . . . . . N

Compounding period [year] . . . . . n

Plant capacity, mass flow basis . . . . . Capacity

Rate of return . . . . . r

Reactor temperature . . . . . T_{reactor}

Revenue . . . . . R

Solid phase . . . . . $(_s)$

Standard Gibbs free energy . . . . . g^o

Temperature . . . . . T

Temperature . . . . . T

Thermal energy recovered from waste streams . . . . . $\dot{Q}_{\text{recovered}}$

Universal gas constant . . . . . R_g

Vapor pressure . . . . . P

Year (cost analysis) . . . . . t

LIST OF ABBREVIATIONS

Cold gas efficiency	CGE
Community Power Corporation	CPC
Electrical revenue	elec
Heat Exchanger	HX
Higher Heating Value	HHV
Lower Heating Value	LHV
Manufacturing cost	mfg
Minimum Acceptable Rate of Return	MARR
MGD	Million Gallons per Day
Nitrogen Oxides	NO_x
Wastewater Treatment Plant	WWTP
Present Worth	PW
Pressure Swing Adsorption	PSA
Relative Error	RE
Sulfur Oxides	SO_x
Thermochemical Conversion	TCC
Total Capital Investment	TCI
Total Purchased Equipment Cost	TPEC
Weight percent	wt %

ACKNOWLEDGMENTS

I would like to thank Dotti Ramey and Dr. Tzahi Cath of Civil and Environmental engineering for bringing this project to myself and Dr. Porter and for their help in understanding wastewater treatment. I would also like to thank Dr. Robert Braun for his advice in systems analysis, and my advisor Dr. Jason Porter for his invaluable guidance.

To my grandfather, John Gharst.

CHAPTER 1
INTRODUCTION

Wastewater treatment sludge, 'sludge', is a dilute suspension of micro-organisms, noxious organic matter, and mineral species in up to 99% water. Sludge is produced at a rate of about 250 mg/L of mixed municipal and light industrial wastewater treated [1]. In 2005, about 8.2 million dry tons of sludge was produced in the United States. Sludge production was seen to increase 29% faster than the U.S. population growth [2]. Management of this process effluent can present a financial and environmental challenge for wastewater treatment plants, WWTPs. Operators of small urban WWTPs see the greatest challenge as their operations do not benefit from economies of scale which permit larger facilities to absorb the costs and plant footprint of microbial sludge stabilization schemes. This work considers small scale urban WWTPs, which serve sewage flows of up to 5 million gallons per day (MGD) (0.22 m^3/s).

A contemporary approach to sludge management considers sludge to be a valuable, recoverable resource [3]. On a dry basis, sludge has a lower heating value (LHV) similar to that of low-rank coal, about 15 MJ/kg [4]. This suggests that the value of sludge might best be recovered as a fuel for on-site electricity generation. Thermochemical conversion (TCC) technologies subject sludge to chemical processes at high temperatures to convert the chemical energy in sludge into heat, more useful fuels, or both. To date, no small scale (<100 kW) techno-economic analyses of TCC-power generation have been found in the literature for wastewater sludge or other biomass fuels. This study intends to determine the feasibility of applying thermochemical techniques to wastewater sludge from a system level perspective.

Four candidate TCC technologies were looked at in this study: wet oxidation, direct combustion, pyrolysis, and gasification (air blown, steam blown, and supercritical water). The technical and economic aspects of these TCC technologies are considered with a view

toward the unique demands of small-scale, decentralized wastewater treatment plants. A model generating plant incorporating the most appropriate TCC process is simulated in the process modeling software ASPEN Plus®. The systems are then analyzed for technical feasibility with currently available technology. Data from the simulations are used to inform an economic model which compares each process to a base case of thermal drying and landfill disposal to determine the WWTP plant capacity for which TCC based generation is economically viable.

1.1 Previous Work

Numerous works are available describing TCC technologies applied to wastewater sludge and biomass in general; although nearly all the literature found considers only large installations and gives only a general overview of the technology. Werther and Ogada [4] published the often cited work *Sewage Sludge Combustion*. While their paper focuses on combustion systems, the authors describe anaerobic digestion and many TCC processes. Other studies [5], [6] investigate the application of TCC processes to wastewater solids; however technical and economic feasibility are not discussed. Rulkens [7] work performs a high-level review of various biological and chemical processes including research-stage processes like biological fuel cells. Little detail is provided about the practical application of these technologies to WWTPs. Bridgwater [8] provides a technological assessment of TCC technologies but gives no systems analysis. Houillon and Jolliet [9] conduct life cycle analyses on a variety of solids management schemes from land application to incineration. Their analysis neglects gasification, and they provide no detailed information about their system models. Furness and colleagues [10] provide a good description of TCC technologies but perform no systems analyses. Manara and Zabanioutou [11] include technological feasibility and environmental impact of TCC technologies but lack an economics evaluation. Some studies [12] investigate the production of biodiesel or other fuels from separated sludge lipids. Other studies, [13], [14], [15] focus on TCC of common biomass sources such as wood, municipal solid waste (MSW), and agricultural products to either fuels or electricity. None of the review works

found specifically consider small-scale wastewater treatment scenarios.

Many authors have published systems level and techno-economic analyses of biomass TCC into fuels or electricity for larger systems. Braun, Swanson, and others [16], [17] examine biomass gasification systems but focus primarily on large bio-refineries. Gribik and colleagues [18] worked on wood hog fuel systems for industrial process heat. Mann and Spath [19] conducted a thorough life cycle assessment of large biomass gasification power plant, although their plant capacity is central utility scale, processing 1334 dry metric ton/ day. Small scale works by Choy [20] and Arena [21] provide systems level detailed techno-economic analyses of biomass gasification systems. However, even in these cases a small system is considered to operate on 10 dry tons/day compared to the maximum of 5 dry tons/ day considered in the present study. Their systems models are only general, they do not describe optimization or sensitivity to fuel characteristics. Arjharn and colleagues [22] published a study on a small-scale (2.4 dry ton/ day) sludge fueled pilot gasification plant. Their work however focused on optimization of gasifier operating conditions, not net power optimization or economic considerations. Crucially, they did not consider the energy requirement to dry sludge.

No literature found to date provides both a system design and techno-economic analysis of small scale ($<$ 10 ton/day fueling rate) biomass TCC cogeneration systems. The present study concentrates specifically on sludge however the system design and modeling should be applicable to a variety of biomass fuels with appropriate calibration to experimental data.

1.2 Wastewater Sludge Characteristics

Technical fuels are commonly described by their proximate and ultimate analyses. Table 1.1 gives the composition of the sludge used in this study along with common bio-resource fuels. The two most obvious differences between sludge and more common biofuels are initial moisture and ash content. A great difficulty in exploiting sludge as a fuel is the need to remove substantial quantities of water. Simulations predict that up to 60 % of the chemical energy in dried sludge is required for thermal drying to a point useful for most thermo-

chemical processes. Ash presents other challenges to thermochemical conversion of sludge, particularly corrosion. Sludge contains more ash than other biofuels mostly due to the upstream wastewater treatment process. Essentially all material which cannot be metabolized by bacteria is concentrated in sludge.

The sludges studied by Ramey, et. al [23] contain (on a dry basis) 1,829 mg/kg Na, 5,354 mg/kg K, and 19,603 mg/kg Ca (average of all specimens). Ash can be aggressively corrosive at high temperature [24]. Ash high in Na and K salts may also provide a benefit to the system by catalyzing tar cracking reactions at high temperatures, typically in excess of 500 °C [25, 26]. A further complication of sludge not represented by proximate and ultimate analyses is heavy metals content, including Cd, Hg, Pb, and Zn. At flame temperatures achieved during sludge or char combustion metals may vaporize and entrain with the exhaust gas stream. Metals remaining in ash and char may also be leached acidic water [6, 27]. Otherwise, the elemental composition of sludge is generally similar to the other materials listed. Due to the presence of fats, oils, and greases, the oxygen mass fraction of sludge is somewhat lower, which partially offsets the lower mass-basis heating value due to ash content. Nitrogen is also significantly greater owing to the presence of proteins in sludge which are a minor species in ligno-cellulosic biomass.

1.3 Current Sludge Management Practices

In the United States, resource recovery efforts promoted by the U.S. Environmental Protection Agency focus exclusively on land application of stabilized sludge to recover nutrients [31]. Approximately 55% of sludge generated at WWTPs is land applied to agricultural, forest, and disturbed lands [32]. To prepare sludge for land application, stabilization is required to reduce or eliminate pathogens and vector (disease carrying organism) attraction. Similar stabilization is required for landfill disposal. Biological treatment is accomplished using aerobic or anaerobic digestion; energy recovery is only possible from anaerobic digestion. Physical treatment using thermal or pH adjustment methods are also acceptable stabilization technologies [33]. Thermal means generally involve pasteurization or drying to

Table 1.1: Biomass fuel chemical characteristics. Yields are dry wt. % unless otherwise indicated.

Analysis	**Wastewater Sludge**[1]	**Pine Wood**[2]	**Corn Straw**[3]	**Municipal**[4] **Solid Waste**
Initial Moisture (Wet Basis)	80 (Dewatered)	12	6.17	8.8
Fixed Carbon	9.03	16	13.75	11.79
Volatile Matter	71.3	71.5	75.95	82.8
Ash	19.67	0.5	5.93	5.9.
C	42.92	51.6	43.83	51.81
H	6.04	4.9	5.95	5.76
O	24.51	42.6	45.01	30.22
N	5.91	0.9	0.97	0.26
S	0.95	Not Detected	0.13	0.36
LHV [MJ/kg]	16.7	20.2 (HHV)	17.75	21.3

[1] [23] [2] [28] [3] [29] [4] [30]

$<$ 10 wt % water. Physical methods do not allow for energy recovery and are not considered further. The energy requirements to prepare sludge for land application is reported to be approximately 15 % of WWTP energy use under current solids management strategies [31].

Anaerobic digestion is appropriate for WWTPs with flows greater than 5 MGD [1], and approximately 50 % of the WWTPs with flows greater than 5 MGD employ anaerobic digestion for sludge stabilization. The anaerobic digestion process allows bacteria to operate on sludge under anoxic conditions and elevated temperatures, around 35 °C, and contact times that can exceed 20 days [34]. Microbial action converts a fraction of the sludge volatile organic content to a combustible biogas. A substantial volume of stabilized biosolids slurry remains for downstream disposal. The contact time requirement demands large reactors and holding tanks. Such tankage requirements are doubly disadvantageous for anaerobic digestion in decentralized urban WWTPs. First, the WWTP must accept the urban real-estate cost for the tankage. Second, heat losses from the large surface area tanks may require substantial heating duty despite the relatively low operating temperatures, especially in cool climates.

Biogas produced in anaerobic digestion processes is a mixture of 40-60 mole % CH_4, with the balance composed of CO_2 and minor species including H_2S and siloxanes (organic silicon oxides). Anaerobic digestion captures 20-40 % of the energy initially present in the feedstock as LHV_{biogas} [34]. Biogas from anaerobic digestion would be expected to have a LHV between 3.3 and 6.7 kJ/kg for the sludge studied in this work. In WWTPs, a portion of the produced biogas is typically fired in a boiler to heat the digesters, making the stabilization process thermally self-sustaining. Fired in an internal combustion engine at 25 % efficiency, anaerobic digestion can convert between 5 % and 10 % of the initial chemical energy in the sludge into shaft power. In over 80 % of the plants employing anaerobic digestion excess biogas is flared without energy recovery [1]. It is clear that anaerobic digestion is employed more for sludge stabilization than energy recovery.

Recycling through land application provides a means of recovering macro-and trace nutrients from wastewater solids. If wastewater solids are stabilized using anaerobic digestion, energy recovery is possible, but rarely realized. While recovery of nutrients has been largely realized through land application, recovery of energy remains elusive for most WWTPs. In this regard, TCC may represent a better option for energy recovery from wastewater sludge.

1.4 Alternative Uses for Wastewater Sludge

Aside from the nutrient-recovery-based beneficial use schemes described in Section 1.3, other uses for sludge are available. In many cases the sludge or ash is used in the production of cementicious building materials. The ash from sludge combustion can be added as an aggregate in cement, brick, and cement-based mortar formulations [6, 7, 35]. Dried sludge is doubly beneficial to cement kilning operations. Dried sludge can be combusted at up to 5 % of the cement works' clinker production capacity providing a carbon-neutral supplementary fuel. Combustion ash can then be recycled into the finished cement as an aggregate for concrete. Care must be taken by the building material manufacturer to ensure sludge ash composition is compatible with the final cement, concrete, brick, or mortar product. Fytili and Zabaniotou [6] describe some of the effects that common sludge species have on concretes. Free lime (reactive CaO) and chlorides can accelerate hardening of concretes. Chlorides also promote corrosion of reinforcement steel. Alkali species in general increase the risk of cement cracking. Phosphate as P_2O_5 reduces final strength.

From an environmental standpoint, incorporating sludge ash in cement can stabilize most heavy metals against leaching. However, up to 98 % of the initial Hg in sludge is found as vapor in hot flue gas if sludge is fired as a fuel [4, 6]. Kilns which burn municipal solid waste and coal are likely to have appropriate stack gas cleaning facilities. Hg should not pose a problem to such operations. Ash as a product of TCC at the WWTP site may retain nearly all the initial Hg. Incorporation of TCC ash into cement formulations stabilizes Hg so long as the ash is blended after kilning [4].

1.5 Thermochemical Conversion Technologies

Thermochemical conversion (TCC) processes are routinely used to transform solid fuels into heat or a more valuable technical fuel such as synthesis gas or bio-oil [4, 6, 15] For consideration in this study, candidate TCC technologies must be at least in the pilot plant stage of development and able to support the production of electricity on-site. Literature review suggests wet oxidation, direct combustion, pyrolysis, and gasification may be appropriate TCC technologies. A short summary of these technologies with a view to decentralized WWTPs is presented.

- **Wet Oxidation.** Wet oxidation is an exothermic process which takes place in an oxygenated aqueous phase at pressures from 5-30 MPa and temperatures of about 150 °C-600 °C. Organic species are oxidized to H_2O, CO_2, NH_3, volatile fatty acids, and solvents [36]. Wet Oxidation is principally concerned with stabilization of hazardous organic waste streams. The process in wastewater treatment is intended to make inorganic and hazardous organic waste material in dilute aqueous suspensions easily settleable and filterable for disposal as solid waste [37]. Wet oxidation is easily eliminated as a candidate TCC process as it cannot produce electrical power. A wet oxidation process in a U.S. wastewater plant described by [38] is capable of supplying process heat at only 115.5 °C. No evidence has been found of a wet oxidation process producing electricity. Considering the low operating temperatures it is not possible to efficiently raise steam for a Rankine cycle. Additionally, the process effluent does not include any useful fuel species.

- **Combustion and Incineration.** Direct combustion involves burning sludge in a furnace in order to decompose hazardous organic material, concentrate ash, and produce high temperature flue gas [4]. Incineration of sludge has a long history as a waste stabilization mechanism, although energy recovery from incineration of sludge in small scale installations has not been found in this literature search. Often, wastewater

sludge incinerators require supplementary fuel due to drying heat loads and surface heat losses from the large furnaces [4]. One of the greatest challenges in sludge combustion is stack emissions control. Emissions include fly ash, SO_x, NO_x, HCl, Hg, Cd, dioxins, and furans [6]. Remediation of these emissions requires capital intensive stack gas cleaning facilities [39]. A further disadvantage is the low efficiency that can be expected from a small Rankine cycle system. Bridgwater [15] notes that small scale facilities can expect to achieve 15% electrical efficiency, a claim supported by Brown [40].

Another possible mode of sludge combustion, co-combustion, involves burning dried sludge as an amendment to a utility fuel such as coal. Sludge must be pre-dried and conveyed to the utility plant. As co-combustion does not produce on site power it is outside the scope of this analysis. Direct combustion is limited by stack emissions considerations, cost, and efficiency. Sludge combustion literature describes large-scale installations; only the largest of which recover heat for a Rankine power cycle [7], [39]. It is expected that the cost of boiler, turbogenerator, and heat rejection equipment in addition to stack gas scrubbing facilities would be overwhelming for a small scale WWTP.

- **Pyrolysis.** Fast pyrolysis of sludge heats the solids stream to elevated temperatures, 450 °C-750 °C, in an inert environment, usually circulating flue gas or pyrolysis gas. Heat-driven chemical reactions volatilize and thermolyze organic species into low molecular weight gases (H_2, CO, CO_2, lower hydrocarbons) and smaller reactive organic moieties which may recombine into a condensable vapor. The process produces three fractions, a sold char composed of unreacted carbon and ash, an oily water-miscible liquid (bio-oil), and a combustible gas [41]. Fast pyrolysis refers to gas residence times under about 2.5 seconds which encourages liquid production by reducing the time available for thermal cracking and steam reforming reactions to convert oil precursors into permanent gases. Pyrolysis processes are typically operated to maximize bio-oil yield.

The oil, once refined, is easily stored and transported [42].

Reactor conditions can influence how the products partition into each phase. Ash tends to catalyze cracking of oil precursors into gas species. The high ash content of sludge results in maximum oil yields of about 50 wt% [27]. Char gasification (see reactions 1.1a-1.1g) is restricted at the relatively low temperatures needed for maximum oil yield, reducing overall efficiency. Char yields above 30 wt% are not uncommon [43]. At high temperature, a portion of the condensable vapors can be further reformed into H_2, CO, and CO_2 within the reactor by the water-gas shift and steam reforming reactions. Gas yields up to 70 wt% are possible although the overall process efficiency of high temperature pyrolysis is less than that of gasification [44].

Pyrolysis oil from sludge is thick, corrosive, water laden and shows poor combustion characteristics [45]. As of 2013 pyrolysis oil produced from sludge has not been demonstrated as an effective reciprocating engine fuel without extensive physical and chemical upgrading [46, 47]. In particular, the water content of bio-oil produced from sludge creates difficulty in achieving stable ignition in compression-ignition engines [45, 48]. However, pyrolysis bio-oil has been demonstrated to fuel combustion turbines [49].

It may be possible to satisfy the heat and hydrogen demands of a hydrocracking and hydrotreating process using pyrolysis gas. A portion of the pyrolysis gas can be combusted directly for heat and the remainder steam-reformed to produce hydrogen. However the energy expenditure for chemical upgrading is not justified for on-site electrical generation where simple physical cleaning processes can allow gasification syngas to fire reciprocating engines and combustion turbines [50].

In the case of sludge, pyrolysis produces three phases of fuel product, each with a significant fraction of the initial feedstream energy. Char combustion suffers the same drawbacks as direct combustion, notably stack gas cleaning [27, 39]. Operating a pyrolysis process to maximize gas production converges to the conditions of steam

gasification. Due to its ability to produce a storable liquid fuel product, fast pyrolysis is usually considered for liquid biofuel production [42]. Overall, pyrolysis represents a better value proposition for producing transportation fuel in large scale biorefineries which can efficiently integrate bio-oil upgrading.

- **Gasification.** Gasification is the process of converting carbonaceous feedstock into a combustible synthesis gas, syngas, via partial oxidation in a net reducing atmosphere at high temperature [51]. Gasification in practice can be broken into four distinct processes: fuel drying and devolatilization, pyrolysis, solid carbon gasification, and gas-phase reactions (mainly water-gas shift and the steam reforming reactions) [52]. As fresh fuel is heated, moisture and light organic molecules evaporate, drying the fuel. At temperatures greater than about 400 °C pyrolysis reactions occur. Heavier organic molecules evaporate from the solid char and begin to participate in gas phase reactions [53]. Large molecules are thermolyzed into simpler species which may be reactive and re-combine. Common species in this phase of gasification are H_2, CO_2, CO, H_2O, CH_4, C_xH_y, where x, y are small numbers, solid carbon, as well as reactive cations, HCN, C_3H_3, and carboxylic acids and aldehydes [54]. The precise set of reactions which transform the above mentioned species, and others not listed, is not well known [28]. However, pure pyrolysis processes (lower temperatures, anoxic) produce a bio-oil composed of oxygenated hydrocarbons [55] which may be converted through the steam reforming reaction, 1.1f, to simpler syngas species such as H_2, CO, CO_2, H_2, and CH_4. The solid carbon char remaining after devolatilization and pyrolysis is transformed into a gas via the reactions 1.1a-1.1g [28],

  Oxidation

$$C + O_2 \rightleftharpoons CO_2 \quad (-111 \text{ MJ/Kmol}) \tag{1.1a}$$

$$C + \frac{1}{2}O_2 \rightleftharpoons CO \quad (-283 \text{ MJ/Kmol}) \tag{1.1b}$$

Boudouard

$$C + CO_2 \rightleftharpoons 2CO \ \ (172 \text{ MJ/Kmol}) \tag{1.1c}$$

Water- Gas Reaction

$$C + H_2O \rightleftharpoons CO + H_2 \ \ (131 \text{ MJ/Kmol}) \tag{1.1d}$$

Methanation

$$C + 2H_2 \rightleftharpoons CH_4 \ \ (-75 \text{ MJ/Kmol}) \tag{1.1e}$$

Water- Gas Shift

$$CO + H_2O \rightleftharpoons CO_2 + H_2 \ \ (-41 \text{ MJ/Kmol}) \tag{1.1f}$$

Steam Reforming

$$CH_4 + H_2O \rightleftharpoons CO + 3H_2 \ \ (206 \text{ MJ/Kmol}) \tag{1.1g}$$

The reversibility of gasification reactions must be stressed. The forward combustion reactions 1.1a and 1.1b are highly thermodynamically favorable, with standard enthalpy changes of -111 MJ/Kmol and -283 MJ/Kmol respectively. High temperatures must be reached before the forward rates of reactions 1.1c, 1.1d, and 1.1g contribute substantially to global gasification chemistry. Thus gasification must occur at high temperature. Furthermore, per the principle of Le Châtlier, the effect of increased pressure is to drive a reaction or set of coupled reactions in the direction which reduces the total number of moles involved in the reaction. High pressures should thus increase the conversion of solid carbon (reactions 1.1a, 1.1b and 1.1e) and suppress 1.1g. As

sludge, and biomass in general, tends to have a low fixed (solid) carbon fraction (see Table 1.1) the gain in solid carbon conversion at increased pressure does not justify the cost and complexity of a pressurized reactor. Thus sludge gasification is conducted at or near atmospheric pressure [22, 56, 57] which allows for simpler and less expensive reactor construction.

Gasification of sludge takes place at temperatures from 750 °C-1100 °C [58]. The reactions 1.1a-1.1g produce a fuel gas composed of H_2, CO, CH_4, CO_2, H_2O, N_2, minor species, and tars [28]. Tars can be considered the products of pyrolysis which have not been reformed into syngas. The reactions 1.1a-1.1g are net endothermic under a molar C/O ratio near unity. Thus, a heat source must be supplied to drive the gasification process. Heat can be transferred from an external source, or supplied internally by partial combustion of the fuel by admitting molecular oxygen in the form of air or pure oxygen gas.

Three oxidants are commonly used in gasifiers: air, pure oxygen, steam, or a mixture of steam with either air or oxygen. Air blown gasification admits less than a stoichiometric quantity of air to burn a portion of the fuel to satisfy endothermic gasification reactions. This process can be mechanically simple and has been applied commercially at small scale to a variety of fuels [59]. A major disadvantage of air-blown gasification is that atmospheric nitrogen from the combustion air acts as a diluent, reducing the syngas heating value and increasing reactor heat duty. Lower heating values (LHV) for air blown gasification are about 4-6 MJ/kg [15]. Steam blown gasification admits no air; instead oxygen for the chemical reactions is supplied by steam. Steam blown gasifiers require an external heat source. The advantage of steam blown gasification is a greater syngas LHV, 15-20 MJ/kg. Additionally, steam gasification tends to show superior carbon conversion and tar reduction [28]. Oxygen blown gasification has an intermediate LHV at 10-12 MJ/kg [15] and generally the cleanest syngas with regard to tars.

Oxygen blown reactors do not have the heating demands of raising steam to reactor temperature although the oxygen separation plant can consume substantial energy. Oxygen blown gasification was not treated rigorously in this analysis due to uncertainties regarding the scaling of oxygen separation apparatus to small systems. Raw syngas contains tars and contaminant species (H_2S, HCl) which must be scrubbed before use as a fuel. Numerous sources [60], [61], [19] suggest that bag filtration and a water scrubber produce a gas suitable to fire an spark-ignition engine or combustion turbine.

- **Supercritical Water Gasification.** Supercritical water gasification processes operate above the critical point of water, 22.1 MPa, and temperatures up to 1000 °C [62]. The supercritical process offers some unique advantages related to the nature of supercritical fluids. The hydrogen bonding which characterizes the excellent ability of liquid water to dissolve ionic compounds and reject organic compounds is disrupted [63]. Typically hydrophobic molecules such as hydrocarbons become soluble while many ionic compounds do not dissolve. The solubility of organic material improves contact with the gasification medium, supercritical water, enhancing product yield. Ash and corrosive salts remain suspended in the medium and can be removed from the reactor through a purge valve [64]. Additionally, a particularly useful advantage is that the process does not require a dry feedstock. Despite these advantages, significant challenges remain. Supercritical water is itself quite corrosive. Common materials resistant to corrosion in sludge service are not capable of supporting the pressure stresses at supercritical conditions [63]. Reactors must be built of expensive precipitation hardening steels or similar materials. While tars are not produced in significant quantities under reactor conditions, pilot plant experience has noted difficulties with tars occluding process orifices due to slow heating as the feedstream approaches the furnace [64]. Further difficulties are encountered feeding slurries into a reactor at high pressure [65].

  Supercritical water gasification must be excluded due mostly to its state of development. An important consideration in supercritical water gasification is heating the wet

sludge to gasification temperatures. Net energy recovery depends on highly effective thermal integration. [65]

Selection of the most appropriate TCC for electricity generation by decentralized wastewater treatment plants is based not only on thermochemical characteristics but also on energy efficiency, environmental considerations, and applicability to small scale installations. Since the goal of waste to energy systems is to electrical power, it is of prime importance that the process provides either a useful fuel stream or sufficient heat at an appropriate temperature to produce net power after satisfying parasitic loads. Air-and steam-blown gasification suffer from none of the drawbacks described for the competing TCC technologies. Gasification has been demonstrated for a variety of biomass sources, including sludge [22, 56, 57]. Thus air or steam blown gasification are considered to be the only TCC processes suitable to decentralized wastewater treatment scenarios. No clear advantage is found between air and steam blown gasification from a qualitative comparison. The greater LHV of steam process syngas may be offset by the heating duty to raise steam to reactor temperature. Therefore both systems are simulated to compare net electrical and thermal output and technical feasibility.

1.6 Research Objectives

This research effort was intended to find the minimum WWTP capacity for which electric power generation from sewage sludge is feasible using air or steam gasification as a front-end technology. Feasibility of a process was defined as the ability to produce on-site electrical power from currently available technology while presenting an economically viable business case. In order to test for overall feasibility, three separate analyses were conducted, each intended to answer whether sludge fueled generation is energetically, technically, and economically feasible.

The overall structure of the analysis is shown in Figure 1.1. Raw sludge flow rate (representing WWTP capacity) was varied into the model system. Simulations determined material and energy flows both across the system boundary and around every component.

These data were coupled to the economic model in order to determine the costs and revenues of the proposed system. The system design and optimized operating conditions were coupled into the technical analysis to determine whether such a system could indeed be built.

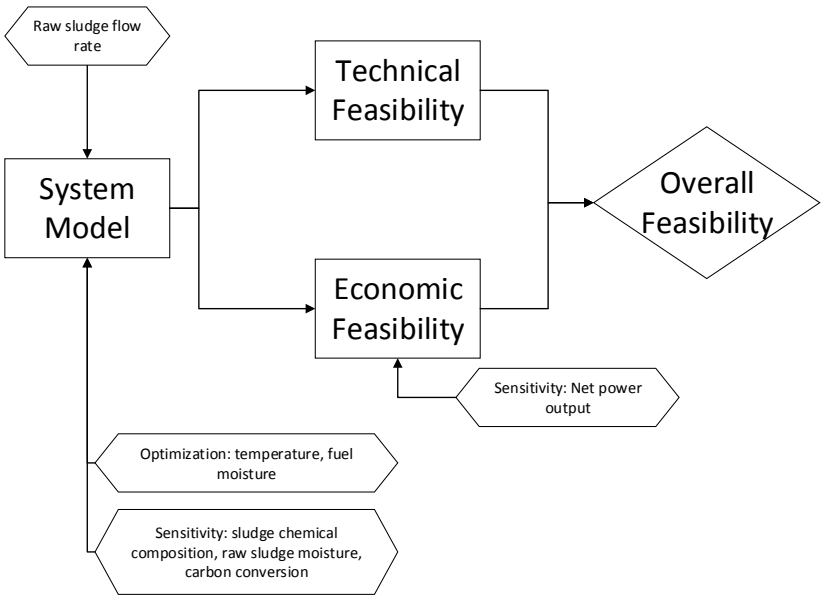

Figure 1.1: Research flow sheet. Variables are shown in hexagons, feasibility analyses in rectangles, and overall feasibility in the rhombus. Generally, raw sludge flow rate is varied to determine the minimum WWTP capacity for which a gasification-generation plant is feasible. Optimization variables determine system operating conditions and sensitivity variables study the effect of the variables on overall feasibility.

Energetic feasibility was tested by designing and optimizing a model system for both air and steam gasification processes. The temperature and fuel moisture conditions for each system were optimized by parametric studies maximizing net power output. While these parameters needed to be fixed to perform the energetic analysis, they were considered part of the research effort due to their effect on technical feasibility. The optimized conditions found in the energetic feasibility are only truly feasible if they are within the capability of available

technology. Further studies on the models tested the sensitivity of overall feasibility to fuel chemical composition, raw sludge moisture, and carbon conversion efficiency, (see Section 2.4), using the optimized system model. It should be noted that the sludge composition given in Table 1.1 was used for all results reported in Section 3. Sensitivity studies only looked at the effect changing the various parameters has on overall feasibility. The energetic feasibility analysis was also used to conclude that the air process is substantially superior to the steam process, from a net power perspective.

Technical feasibility was determined by considering the operating conditions of the gasifier plant. In particular, whether technologies exist that can handle and convey semi-dry sludge and whether components (such as heat exchangers and blowers) are available which can tolerate the corrosive nature of hot, wet syngas. Economic feasibility was tested by comparing the costs and revenues of the gasification plant to those of a base case, thermal drying and landfill disposal (see Section 2.8.) The economic model accepted cost data from various sources however these were not specifically treated as variables. A sensitivity analysis was conducted to determine the effect on net power output on economic feasibility. Both the technical and economic feasibility conclusions were entirely informed by the system models.

CHAPTER 2

METHODS

Effective thermal system design is an exercise in balancing thermal integration, energy output, and cost. In the case of wet fuel, such as wastewater sludge, the greatest process energy demands are drying the fuel and heating it to reactor temperature, 850 °C. Figure 2.1 demonstrates these energy requirements as a function of the final moisture content (post-dryer). The energy scale is normalized to sludge infeed energy as $\dot{Q}/(\dot{m}_{\text{sludge}} LHV_{\text{sludge}})$ where $\dot{Q}$ stands for a heat duty. Up to 60% of the dry sludge LHV is required to thermally dry sludge initially received at 80 wt% moisture post-centrifuge.

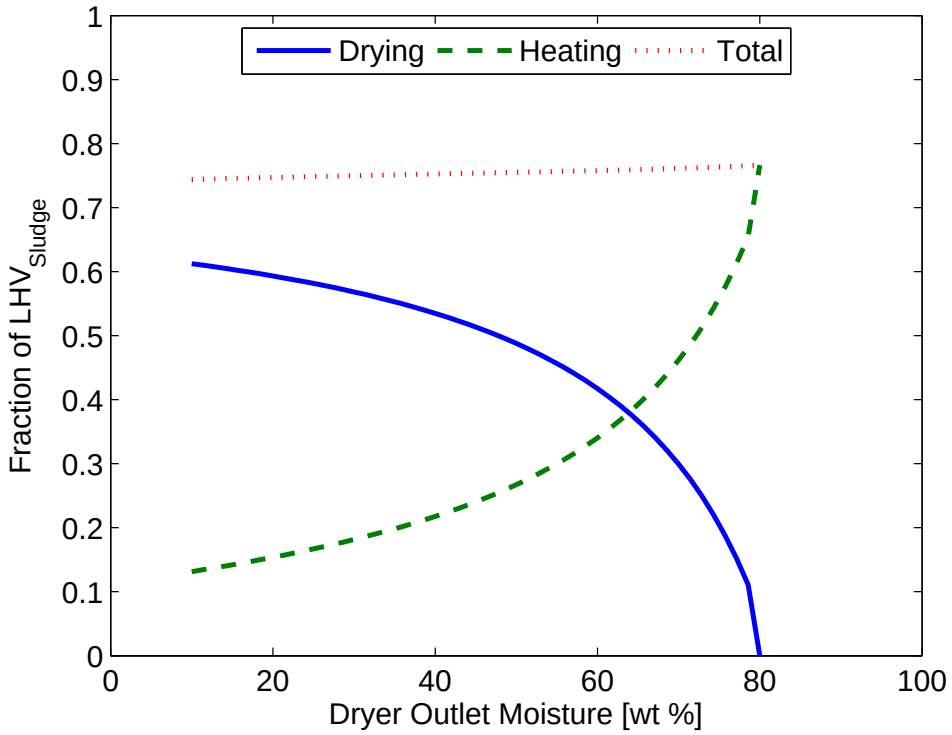

Figure 2.1: Energy required to dry and heat sludge to 850 °C. Drying energy is calculated as Δh_{fg}. Heating energy is calculated using the ASPEN Plus *HCOALGEN* property model. The ordinate scale is heat duty normalized by $\dot{m}_{\text{sludge}} LHV_{\text{sludge}}$

Further energy is expended heating the fuel to reactor temperature. In total, about 75 % of the fuel energy coming into the system must be applied to drying and heating the fuel. Thus, heat recovery and thermal integration are of primary importance to the system design.

Additional complications in sludge-fueled systems arise from environmental considerations. The wastewater treatment process concentrates heavy metals (including Cd, Hg, Pb, and Zn) in sludge, which tend to be associated with char particles [66]. Char combustion approaches to gasifier heating such as chemical looping combustors risk releasing such metals into an exhaust stream which would then require extensive downstream exhaust scrubbing similar to direct combustion [27, 39]. Therefore this system design does not consider char combustion.

A system design was developed to be simple and cost effective for small scale operation while recovering as much energy as possible for fuel drying (Figure 2.2). The system is composed of four process areas: Convective drying, gasification, gas cooling and cleaning, and spark-ignition engine-generator. Heat recovery is accomplished by recycling all hot gas streams from combustion and syngas cooling to the dryer. This system design is of similar form to those seen in other biomass gasification works [40], [67] suggesting that the overall system design is reasonable. Details of each process area are deferred to Sections 2.1-2.7.

It should be noted that other system configurations may also be effective. WWTPs using a common biological process, activated sludge, have large blower loads for aerating tanks of sewage mixed with recycled microbe-activated sludge [1]. Several considerations including blower load in comparison to gasifier plant generating capacity and local utility feed-in policies may make electrical generation inefficient or burdensome. In particular, if blower loads are on the same scale as electric power output, the irreversibility created in electric generators, switchgear, and variable frequency motor drives may make it more efficient to supply blower loads directly with engine shaft power.

Some further opportunities for thermal integration were not pursued in this design. If less drying energy is needed, efficiencies may be gained by preheating the fuel and air streams

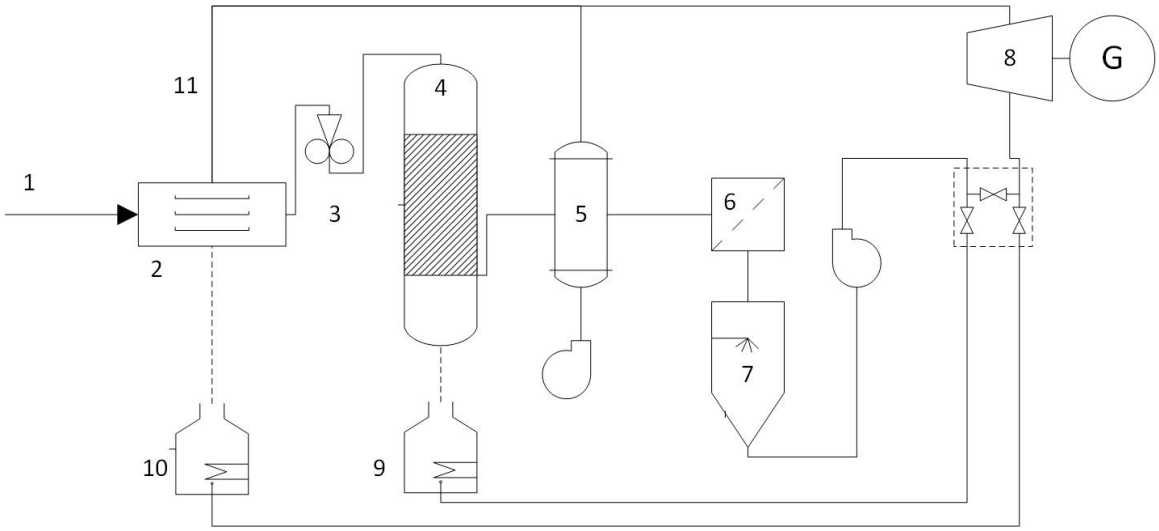

Figure 2.2: Spark ignition engine system flowsheet. 1: sludge feed, 2: dryer, 3: briquetter, 4: gasifier, 5: syngas HX, 6: filter, 7: water scrubber, 8: engine-generator, 9: gasifier heating burner, 10: dryer heating burner, 11: recycled gas streams. Dryer exhaust and various air inlet streams not shown.

entering the gasifier by heat exchange with hot syngas. Such an approach was not attempted in this study. Simulation results revealed that recycled heat streams from combustion and syngas cooling could not satisfy drying loads in all cases leaving little available energy for air preheating.

Another option for energy conversion is to replace the spark-ignition engine with a combustion turbine. Combustion turbines operate in a constant pressure combustion regime which is generally less efficient than the near constant volume combustion regime of spark-ignition engines [68]. However, combustion turbines can accept higher temperature fuel streams than spark ignition engines which are generally limited to around 100 °C to avoid destructive autoignition during compression. Higher fuel temperature allows the turbine to recover sensible energy in the hot fuel stream which otherwise may be wasted or transferred at low temperature. However conventional wisdom suggests that combustion turbines at small scale, less than about 250 kW, are much less cost effective and less efficient than reciprocating engines, especially for low LHV biogas and syngas [69]. For these reasons a combustion turbine was not included in the initial scope of study. However the system model

described in Sections 2.1-2.7 is capable of supporting a combustion turbine. In the interest of fully exploring system design options a turbine based system is built alongside the reciprocating engine based model. A discussion of the net power output of a combustion turbine option can be found in Section 3.5.

The final process option is oxygen blown gasification using pressure-swing adsorption (PSA) oxygen separation. Oxygen blown gasification eliminates the need for inefficient external heating or nitrogen dilution of the syngas stream. The most common approach to oxygen separation for large scale gasifiers is cryogenic separation [52]. However, PSA may present a more economically and energetically viable separation option. PSA operates by flowing pressurized air through a selective adsorption media. At PSA operating pressures the adsorbed gas is sequestered in the adsorption media while less reactive species flow through. Pressure reduction releases the adsorbed gas, regenerating the media. Multiple media canisters are connected in parallel to allow for batchwise-continuous operation. A PSA system operates near ambient (or compression) temperature and pressures in the range of 500-1000 kPa suggesting that energy demands will be less than cryogenic separation. Further modeling effort may be able to address PSA techniques.

2.1 Modeling

System simulation is implemented in the chemical engineering process modeling software ASPEN Plus. ASPEN Plus is well established as a gasification plant modeling tool [70]. Chemistry in ASPEN Plus depends on built-in databanks and equations of state to determine thermophysical properties. The Boston-Matthias modified Peng-Robinson equation of state is used throughout the model [67]. Thermophysical properties (enthalpy, density, specific heat capacity) for sludge and ash are determined from their ultimate and proximate analyses (Table 1.1) by the built-in coal property models *HCOALGEN* and *DCOALIGT*. The coal property models are also appropriate for biomass [71]. Computations are performed using a sequential-modular solver. Recycle streams are nested automatically. The flowsheet used in this modeling effort is shown in Figure 2.3.

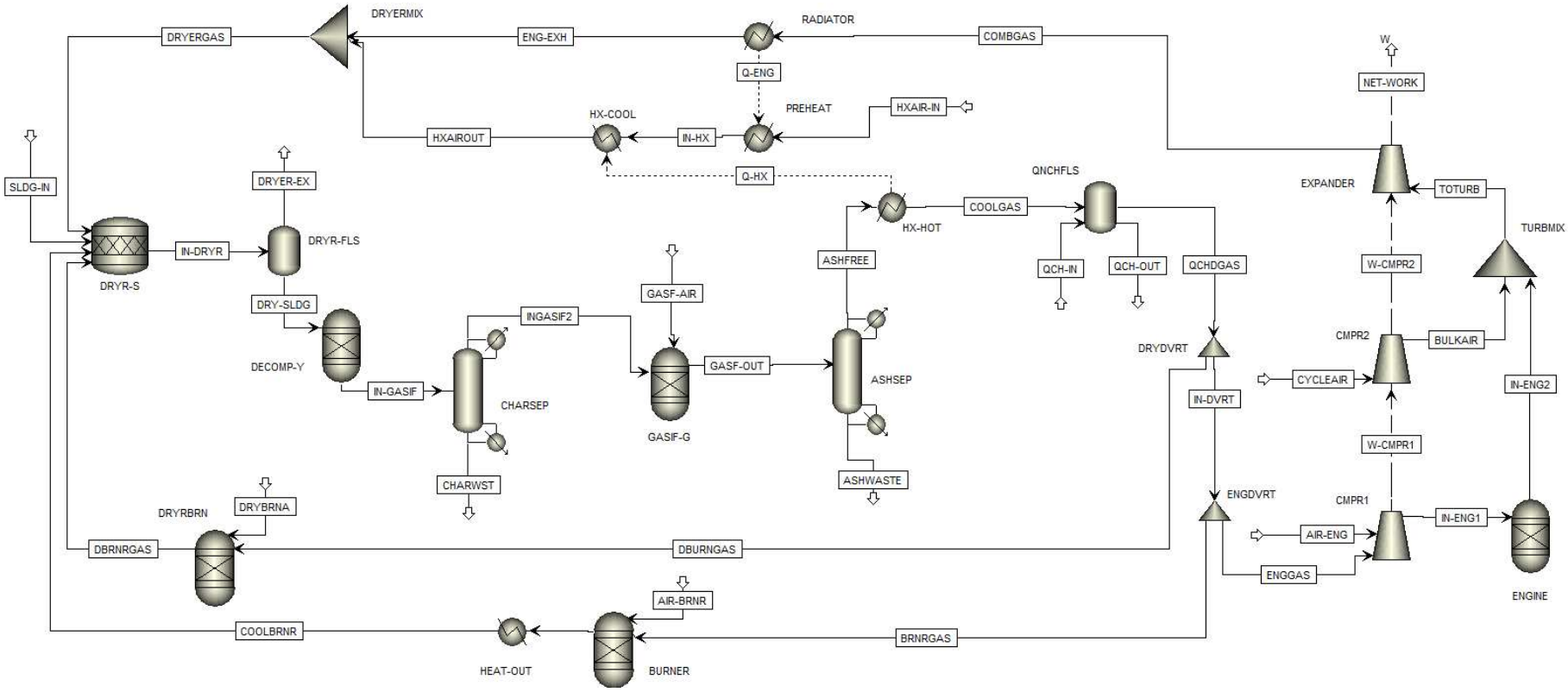

Figure 2.3: ASPEN Plus system flowsheet. Flowsheet includes all unit operations and streams defined in the model. Calculator blocks are not shown.

ASPEN Plus represents physical processes by combinations of unit operations, called *blocks*. Blocks are connected by one-way streams carrying material, heat, and work. Blocks incorporate the physical models necessary to simulate the effect of the unit operation on its inlet material, heat, and work streams. All blocks are specified for thermodynamic variables including temperature, pressure, heat duty and vapor fraction. Additional specifications depend on the unit operation represented by a given block. For example, chemical reactor blocks demand additional specifications such as chemical reactions and kinetic or equilibrium data. Block specifications are described in Sections 2.3-2.7 where appropriate.

Along with unit operation blocks, ASPEN Plus provides computational devices, *Calculator* and *DesignSpec* blocks. *Calculator* blocks accept input variables, which may be any set of flowsheet variables or specifications. Output variables can also be flowsheet variables or specifications and can be used to specify blocks. *Calculator* blocks operate excel files or custom FORTRAN code to calculate output variables. FORTRAN was used exclusively in this modeling effort. *DesignSpec* blocks vary a flowsheet parameter, such as mass flow or temperature, to satisfy a user-defined specification. For example, a *DesignSpec* block in the gas processing area (see Section 2.5) varies the mass flow of cooling air to the syngas heat exchanger to achieve a specified outlet temperature. *DesignSpec* blocks operate by numerically minimizing the first derivative of the system response function to the varied parameter. The Wegstein method was used in all *DesignSpec* blocks to approximate the system response function. Calculator and *DesignSpec* blocks were used throughout the model; they are referenced where appropriate in Sections 2.3-2.7.

All blocks, material, heat, and work streams are shown and labeled in Figure 2.3. The modeling methods described in Sections 2.3-2.7 refer to block names in the flowsheet. *Calculator* and *DesignSpec* blocks are left out of the flowsheet for clarity. The reader should note that the flowsheet in Figure 2.3 is a fully functional general model which accommodates both air and steam processes and both engine and combustion turbine prime movers. Actual simulations of each process were conducted models specific to the system of interest

(air, steam, engine, turbine) in the interest of simplicity as calibration factors and blocks used change for each case. All unit operation blocks, calculators, *DesignSpec* blocks, and specifications except those which apply only to a specific system are otherwise identical. For example, the steam process admits no air to the gasifier. Stream *GASF-AIR* is left out of the steam process model.

2.2 Scope and Assumptions

This analysis is intended to determine the feasibility of producing net electrical power and heat from a general, high level perspective under steady state conditions. The system boundary crosses sludge feed, dryer exhaust, char and ash waste, and net electrical work streams. Sludge is assumed to enter the system at 80 wt% water from upstream mechanical dewatering by centrifuge. As the base case used in the economic model (see Section 2.8) includes centrifugation, mechanical dewatering processes upstream of the system boundary are excluded from the system model. Sludge composition is taken from [23] and shown in Table 1.1. In order to maintain generality, performance characteristics and geometry of individual components are neglected. It is assumed that all components represent real mechanical equipment which is optimized for the mass and energy flows at every point of analysis. Since geometries have been neglected, surface heat losses from all components except the gasifier and engine are also neglected. All components which are unlikely to contribute substantially to the overall plant energy balance are not specifically modeled; a 10 % backwork factor is applied to estimate energy consumption by ancillary equipment. Pressure for all components except the engine is set to 0.1 MPa.

2.3 Dryer

Sludge drying assumes that free water is simply evaporated and the sludge is unaffected except for a change in temperature. No surface effects such as binding energy or crusting are considered. The work of [72] suggests that energy needed to dry sludge is nearly Δh_{fg} of pure water for sludge moisture content between 99 wt% and 10 wt%. The dryer model is a

convective drying process where hot drying gas directly contacts the sludge [24]. Convective dryers are less common in WWTPs, however for situations where relatively low temperature, high mass flow heat streams are available the convective dryer is appropriate [73]. Other drying processes are available, discussion is deferred to Section 3.9.

The sludge dryer consists of a stoichiometric reactor, *DRYR-S*, to convert some weight of sludge to water, vaporize it, and then a flash operation, *DRYR-FLS*, to separate the vapor from dry solids, in similar fashion to [74], [71]. *DRYR-S* is specified as adiabatic with an exhaust vapor fraction of unity. *DRYR-FLS* is specified for adiabatic, atmospheric pressure operation. Simulation of sludge drying begins by converting a fraction of the raw sludge mass to water in *DRYR-S*. The remaining mass is dry (or semi-dry) sludge. Decomposition proceeds according to Equation 2.1

$$\text{Sludge}_{\text{raw}} \rightarrow \text{Conv} * H_2O + (1 - \text{Conv})\text{Sludge}_{\text{dry}} \tag{2.1}$$

The variable *Conv* is a linear factor which determines the mass fraction of sludge which is converted to water. *DRYR-S* operates Equation 2.1 to determine the mass fraction of water to evaporate. The exact value of *Conv* is determined by fixing the moisture content in the dried sludge. An equation relating the final moisture content to initial moisture and *Conv* is created from a mass balance across the reactor.

$$\text{Conv} = \frac{[H_2O_{\text{in}}] - [H_2O_{\text{out}}]}{100 - [H_2O_{\text{out}}]} \tag{2.2}$$

The concentration brackets in Equation 2.2 represent wet basis mass percentages. Equation 2.2 is applied to *RStoic* through a FORTRAN subroutine. Heat for evaporation is provided by a combination of exhaust gas and hot air from the syngas cooler. With the dryer specified as adiabatic and a vapor fraction of unity, the dryer exhaust temperature is exactly $\text{T}_{\text{dewpoint}}$. This specification ensures all water removed from the sludge feed is indeed evaporated. Where heat from recycled gas streams is insufficient to evaporate all water, the dryer records a net heat duty and the system is considered infeasible. Heat in excess of that necessary to evaporate water is manifested as a dryer exhaust stream of $\text{T} > \text{T}_{\text{dewpoint}}$.

Results (Section 3.3) indicate that dryer exhaust temperature at conditions which maximize net power output is sufficiently high to prevent immediate condensation in dryer ducts.

The dryer model assumes simple thermodynamics; free liquid water is simply evaporated by contact with hot gas. The experimental data found in [72] suggest that this is a reasonable approximation from a purely thermodynamic standpoint. However other effects may impair drying kinetics. In particular, the surface of sludge particles may form a hardened crust [75], preventing mass transfer of water from solid sludge particles. The effect may require only mechanical agitation (mixers) to break up the crust, but it is likely that higher temperatures may also be necessary. In keeping with the project scope and assumptions, Section 2.2, component geometry and performance characteristics are not explicitly modeled. General kinetic data are available for sludge drying [72, 75] but without knowledge of the design and residence time of specific drying machinery it is impossible to build a predictive kinetic model. The net effect of the simplified thermodynamic model is that actual drying energy may be greater than simulated energy demand.

Temperatures reached during sludge drying may release volatile organic content (VOC) into the exhaust stream [24]. In practice, a water scrubber is often used to condense VOCs and evaporated water. Scrubbing water may be recycled back to the WWTP headworks without pre-treatment, however such detail is outside the scope of this analysis.

2.4 Gasifier

The gasifier model is built under the assumption that chemistry follows thermodynamic equilibrium. Kinetic and surface chemistry phenomena are neglected. As gasifiers operate at high temperature and relatively long gas residence times (on the order of seconds) it can be expected that thermodynamics dominate chemistry. While this assumption is certainly in error, it is appropriate for simple feasibility analyses [76]. The gasifier model is constructed of two principal unit operations, a yield reactor *DECOMP-Y* and a Gibbs equilibrium reactor *GASIF-G*. The yield reactor models fuel pyrolysis by decomposing sludge into its constituent elements, C, H, O, N, S, ash, and water. A calculator block references the proximate and

ultimate analysis of the infeed sludge to determine the mass-basis decomposition. Most carbon is partitioned into the gas phase except for a portion equal to the fixed carbon mass fraction as determined in the proximate analysis. The solid carbon is represented by graphite. A separation block after *DECOMP-Y* separates a fraction of hot infeed carbon into waste to simulate incomplete carbon conversion. Carbon conversion efficiency, η_c is defined as

$$\eta_c = \frac{m_{C,\text{ feed}}}{m_{C,\text{ syngas}}} \tag{2.3}$$

where m_C is mass flow of carbon. *GASIF-G* then simulates gasification by calculating an equilibrium distribution of reactants and products.

Full chemical equilibrium is an aggressive assumption. An equilibrium restriction was applied to calibrate the model to experimental data. *GASIF-G*, a Gibbs equilibrium reactor, (*RGibbs* in ASPEN Plus terminology) offers two means to restrict chemical equilibrium. The first restricts equilibrium globally by specifying an equilibrium temperature approach, $T_{\text{equilibrium}} = T_{\text{reactor}} + \Delta T_{\text{approach}}$. Equilibrium is calculated at $T_{\text{equilibrium}}$ by minimizing the Gibbs free energy change across the reactor. Global equilibrium restriction only considers products listed as components *a priori*. Such components are expected to be H_2, CO, CO_2, H_2O, N_2, CH_4, $C_{(s)}$, H_2S [56]. Gibbs free energy for an N component mixture is given by Equation 2.4 [77].

$$G = \sum_i^N \chi_i + R_g T \sum_i^N \chi_i \; log \; \chi_i \tag{2.4}$$

where G is the mixture Gibbs free energy, χ_i is a mole fraction of species i, R_g is the universal gas constant, and T is the equilibrium temperature. Differentiating Equation 2.4 with respect to the mole fraction of species i, χ_i, gives the partial Gibbs free energy change

$$\frac{\partial G}{\partial \chi_i} = g_i^o - \sum g_{\text{prods}}^o + R_g T \; log \; \frac{\chi_i}{\sum \chi_{\text{prods}}} \tag{2.5}$$

where sums over subscript $_{\text{prods}}$ refer to any species in the products which contains atoms also present in species i. For example, the Gibbs free energy change with respect to H_2 would have products of H_2 (unreacted), H_2O, CH_4, and H_2S. g^o represents the standard

Gibbs free energy of the species or set of species. N equations of the form of Equation 2.5 are generated and minimized by a least-squares solver. The result of the calculation is a vector of mole fractions of each component considered by the *RGibbs* block. A similar calculation to that in Equations 2.4 and 2.5 proceeds in parallel to determine the phase distribution of all components. At temperatures considered in this analysis all products except ash and unconverted carbon are in the vapor phase.

The second restricted equilibrium method offered by *RGibbs* provides a means to restrict equilibrium by specifying a reaction temperature approach, $T_{\text{equilibrium}}$ for each reaction in a set of linearly independent reactions, $N_{\text{reactions}} = N_{\text{products}} - N_{\text{atoms}}$. Equilibrium is simulated by calculating an equilibrium constant (Equation 2.8) for each linearly independent reaction at $T_{\text{equilibrium}}$. For a general chemical reaction,

$$\alpha\text{A} + \beta\text{B} \rightleftharpoons \gamma\text{C} + \delta\text{D} \tag{2.6}$$

the thermodynamic equilibrium constant is defined as the molar ratio of products to reactants, all raised to their stoichiometric coefficients,

$$K = \frac{[\text{C}]^{\gamma}[\text{D}]^{\delta}}{[\text{A}]^{\alpha}[\text{B}]^{\beta}} \tag{2.7}$$

K can be related to temperature, and the standard Gibbs free energy of reaction, by setting Equation 2.4 for both products and reactants equal to zero. Solving for the equilibrium constant, K, in terms of the right hand side of Equation 2.7, the temperature dependence of chemical equilibrium for ideal, constant pressure systems is found,

$$K = \exp(-\Delta G^{\circ}/R_g T) \tag{2.8}$$

where ΔG° is the standard Gibbs free energy change of reaction. It should be noted that the path from Equation 2.4 to Equation 2.8 transforms mole fractions to partial pressures. With the expression for the equilibrium constant found, calculating the extent of reaction is a simple matter of evaluating Equation 2.8 at $T_{\text{equilibrium}}$. Species not accounted for in the linearly independent reactions are simply passed through to products. Both the global

equilibrium and equilibrium constant approaches were tested during model calibration. The global method was not capable of calibrating the model to experimental data; the equilibrium constant method provided satisfactory agreement with the data. Thus, all simulations were conducted using the equilibrium constant method.

The linearly independent reactions used for this model are

$$CO + H_2O \rightleftharpoons CO_2 + H_2 \tag{2.9}$$

$$C + H_2O \rightleftharpoons CO + H_2 \tag{2.10}$$

$$C + 2H_2 \rightleftharpoons CH_4 \tag{2.11}$$

Restricting equilibrium accounts for kinetic limitations in real systems and allows for calibration to experimental data. A separation block after *GASIF-G* removes hot ash and char from the gas stream into waste, simulating an ash grate.

Tars in gasification describe a heterogeneous group of condensible organic molecules with a molecular weight greater than benzene, 78.11 g/mole [78]. Evolution of tars from sludge gasification may be simulated by including a small number of organic moieties in the gasifier product matrix. Mass spectroscopy data suggest that napthalene, sytrene, xylene, and propane nitrile may be sufficient to represent gasification tars, at least on a mass-evolution basis [58]. However, the representative tar compounds are thermodynamically unfavorable and were not found to be produced by the restricted equilibrium method. Even if representative tar compounds could be produced in the model, the studies used for calibrating $T_{\text{equilibrium}}$ [56, 79] do not include tar speciation and thus validation is not possible. Therefore, tar modeling was excluded from gasification chemistry.

Overall, gasification chemistry is endothermic. Heat for the reactions can be supplied by an external heat source or by partial combustion of the fuel in-situ. The energy balance for the air-blown system is satisfied by a *DesignSpec* block admitting air into *GASIF-G*, simulating partial combustion of the fuel. *GASIF-G* then produces excess heat which is transferred to *DECOMP-Y* at reactor temperature. Air flow is varied until the heat du-

ties of *DECOMP-Y* and *GASIF-G* sum to zero. This approach dynamically calculates an equivalence ratio allowing only the minimum amount of fuel to be burned. For the steam blown system a similar *DesignSpec* block diverts some of the product syngas to a burner. Heat is transferred from hot flue gas to *GASIF-G* at 20 °C above reactor temperature. 20 °C is used as a representative heat exchanger approach temperature throughout the model [80]. Heat in excess of that demanded by *GASIF-G* is further transferred to *DECOMP-Y*. In both cases 3 % of the infeed sludge power $\dot{m}_{\text{sludge}} LHV_{\text{sludge}}$ is added to gasifier heat duty to approximate surface heat losses [70].

2.5 Gas Processing

Raw syngas exiting a gasifier will carry fly ash and char as well as vapor phase tars and must be cleaned. Syngas may be acceptably cleaned to fire an internal combustion engine by bag filtration and a water scrubber [50, 81]. Where water scrubbing cannot remove problem tars or other species by condensation, absorption scrubbing with other fluids (diesel oil, vegetable oil, sulfur adsorbents, etc.) may be used instead of or in conjunction with water scrubbing [82]. Gas processing begins with a 20 °C approach heat exchanger where syngas is cooled to 150 °C. Hot cooling air is recycled to the dryer. The heat exchanger is modeled by a *DesignSpec* block and two heater blocks (*HX-HOT* and *HX-COOL* in Figure 2.3) connected by a heat stream. *HX-HOT* operates on the syngas stream, *HX-COOL* operates on cooling air. Cooled syngas temperature is specified in the *HX-COOL* block. Cooling air mass flow rate is varied by the *DesignSpec* block until cooling air temperature is 20 °C below the syngas outlet temperature.

In order to avoid assuming a particle size distribution and pressure drop, no bag filter is modeled. Instead, solid carbon and ash are removed in separation blocks. A water scrubber then cools the gas to 70 °C, below the condensation point of most tars [24]. Wet scrubbing with water also affects the removal of HCl, NH_3, and mineral ash species incorporating Na and K cations [24]. The scrubber is modeled by the flash operation *QNCHFLS* and a *DesignSpec* block. *QNCHFLS* operates adiabatically at atmospheric pressure. Water use

by the scrubber is not modeled in detail. As stated in Section 2.2, component performance characteristics are neglected. Instead, only the amount of water necessary to cool the syngas to 70 °C is circulated in a closed loop as determined by the *DesignSpec* block. In practice, a certain amount of water will be wasted from the scrubber. Exact water make-up and waste water flows will depend upon the scrubbing apparatus used; although the simulated water consumption needed to cool the gas is on the order of 0.005 kg/s. It may be possible to skim condensed tars off the surface of scrubbing water in a surge tank and recycle them to the gasifier.

In both processes, a portion of the syngas is diverted to fuel burners. Splitter blocks, *DRYDVRT* and *ENGDVRT*, controlled by upstream *DesignSpec* blocks, are used to divert a portion of the product syngas to the burners. Burners are modeled by an adiabatic Gibbs equilibrium block simulating combustion reactions. A calculator block upstream of the burner calculates a stoichiometric air flow rate. Stoichiometry is simulated by Equation 2.12 under the assumption that only H_2, CO, CH_4 participate as fuels in combustion reactions.

$$\dot{y}_{air} = 4.76 * [(\dot{y}_{CO} + \dot{y}_{CH_4}) + (\dot{y}_{CH_4}) - (\dot{y}_{CO}/2)] \tag{2.12}$$

where $\dot{y}$ refers to a molar flow rate and the factor 4.76 accounts for 21 mole % oxygen in air. Burner stoichiometry is set to 10 % excess air.

2.6 Engine

ASPEN Plus does not provide blocks which can accurately simulate a reciprocating internal combustion engine. In particular, the only fluid expander, a turbine block (*Turb*), cannot operate in positive-displacement mode. Additionally, reciprocating engine performance characteristics are heavily influenced by geometry (for example, intake and exhaust valve timing and overlap) which cannot be modeled in ASPEN Plus. Thus, the engine is modeled as a gas turbine (which is easily approximated) and calibrated to the performance of a real spark ignition engine. It is understood that error is introduced by simulating expansion using an isentropic VdP model rather than a polytropic PdV model more representative of a positive

displacement system. Error will also be introduced by approximating the constant volume combustion in a spark ignition engine by constant pressure combustion. These errors are expected to be conservative, underestimating power output. Nonetheless, the overall conclusions of the research effort are not expected to be greatly influenced by this approach. Results (See section 3.10) show that economic feasibility is only weakly sensitive to net power output.

The engine model is built using an assembly of compressor (*CMPR1*), combustor (*ENGINE*), and turbine (*EXPANDER*) blocks [67]. Air and fuel enter the engine at the *CMPR1* block. Combustion stoichiometry is set by an upstream calculator operating Equation 2.12 for stoichiometric combustion. *CMPR1* is specified as an adiabatic positive displacement compressor with a 9.5:1 pressure ratio. 9.5:1 was chosen to approximate a real reciprocating engine compression ratio of 10:1 based on engines used in experimental sludge gasification works [22, 83] along with a technical review of hydrogen fueled internal combustion engines [84]. Combustion is modeled in a Gibbs equilibrium block set to adiabatic operation at the compressor outlet pressure. Hot exhaust is passed through *EXPANDER* to extract shaft work. *EXPANDER* is specified as an isentropic turbine operating adiabatically and exhausting into atmospheric pressure.

Since the modeling effort is intended to estimate the possible net power output of the system such a simple model is justified. Obviously, important effects such as combustion stability, autoignition, volumetric efficiency, etc., are not specifically considered. In particular, the low LHV of air process syngas and high hydrogen concentration of steam process syngas may present operational challenges. Szwaja [83] had difficulty maintaining stable combustion of a syngas produced by air gasification of wastewater sludge. In the case of the steam process, high hydrogen concentration may predispose an engine designed for hydrocarbon fuels to destructive autoignition [84].

In order to approximate the performance of a spark-ignition engine, the engine model was calibrated to match available data. Szwaja [83] finds syngas produced from air gasification

of sludge to be about 22 % efficient in firing a spark ignition engine under a given gas composition. Using the gas composition given in the cited paper, the polytropc efficiency of *CMPR1* and isentropic efficiency of *EXPANDER* were adjusted equally until the engine model converted 22 % of the fuel power as $\dot{m}_{\text{fuel}} LHV_{\text{fuel}}$ into shaft power. Syngas LHV was calculated by

$$LHV \text{ [kJ/kmol]} = \sum_i \chi_i LHV_i \tag{2.13}$$

$$LHV \text{ [kJ/kg]} = LHV_{\text{molar}} / MW_{\text{gas}} = \frac{LHV_{\text{molar}}}{\sum_i \chi_i MW_i} \tag{2.14}$$

for mole fraction χ_i, molecular weight MW_i and reference molar LHV found from Turns' text [68]. Division by the gas molecular weight allows a mass basis LHV to be determined (Equation 2.14).

The polytropic efficiency of *CMPR1* was found to be 91.5 %, the isentropic efficiency of *EXPANDER* was found to be 95 %. Mechanical efficiency was estimated using common figures for mechanical efficiency of low speed engines and was assigned a value of 87 % [85]. Engine calibration was held constant throughout the simulations to allow engine efficiency to vary with gas composition. Alternator efficiency in every case was set to 99 % [86].

2.7 Gas Turbine

While the combustion turbine option was not thoroughly analyzed for technical or economic feasibility, a combustion turbine option was simulated to compare possible net power output and defend the initial choice to use a spark ignition engine as the system's prime mover. The turbine is constructed of a fuel compressor and a bulk air compressor, *CMPR1* and *CMPR2*, an adiabatic combustor, *ENGINE*, and a turbine, *EXPANDER*. For the turbine model, *CMPR1* and *CMPR2* are specified as adiabatic isentropic compressors. *ENGINE*, *EXPANDER* are specified identically to the spark ignition engine model. A stoichiometric quantity of air, set by Equation 2.12, is diverted from the bulk gas flow exiting the air compressor and mixed with fuel in the combustor block (*ENGINE*). Hot combustion gases are

mixed with the remaining high pressure bulk air flow to reduce overall temperature. The mixed gases are directed to the turbine to extract shaft work. A *DesignSpec* block controls the bulk air flow to ensure turbine inlet temperature remains below that of the example turbine's limit, 1100 °C [87]. Combustion turbines may be able to operate on syngas without formal tar removal, especially for low-tar downdraft gasifiers [86] thus the water scrubber is removed from the system for the combustion turbine based plant.

Calibration of the combustion turbine model proceeds in similar fashion to the internal combustion engine, except values for the isentropic efficiencies of the compressor and expander, along with mechanical efficiency, of a representative 30 kW microturbine are available in the literature [87]. The cited study measured turbine performance on a 60 %-40 % mixture of CH_4-CO_2 to simulate landfill biogas. Net shaft power produced by the model turbine was compared against the fuel power, found as $\dot{m}_{\text{fuel}} LHV_{\text{fuel}}$. The compressor and turbine models were adjusted slightly from the manufacturer supplied values to match the 26 % measured efficiency firing biogas at 25 °C inlet temperature. The isentropic efficiencies of *CMPR1, CMPR2* were set at 83 %, the isentropic efficiency of *EXPANDER* set at 84.5 %, and the mechanical efficiency of each component was set to 97 % (as given by the manufacturer.)

A schematic of the gas turbine based system is given in Figure 2.4. Noteworthy changes from Figure 2.2 are the lack of wet scrubber and replacement of the spark ignition engine with the microturbine. In the interest of clarity, air streams not necessary to the visual description of the process are left out of Figure 2.4, but are seen in Figure 2.3.

2.8 Economics

Economic viability is evaluated by calculating the present worth (PW) of the gasification plant option. Present worth discounts net cash flows over the lifetime of the plant to some specified point in time, taken to be analysis year 2010. Positive PW indicates an economically viable business case [18]. Net cash flow is calculated by considering an annual cost difference between the gasification plant and a base case. The base case is thermal stabilization in a

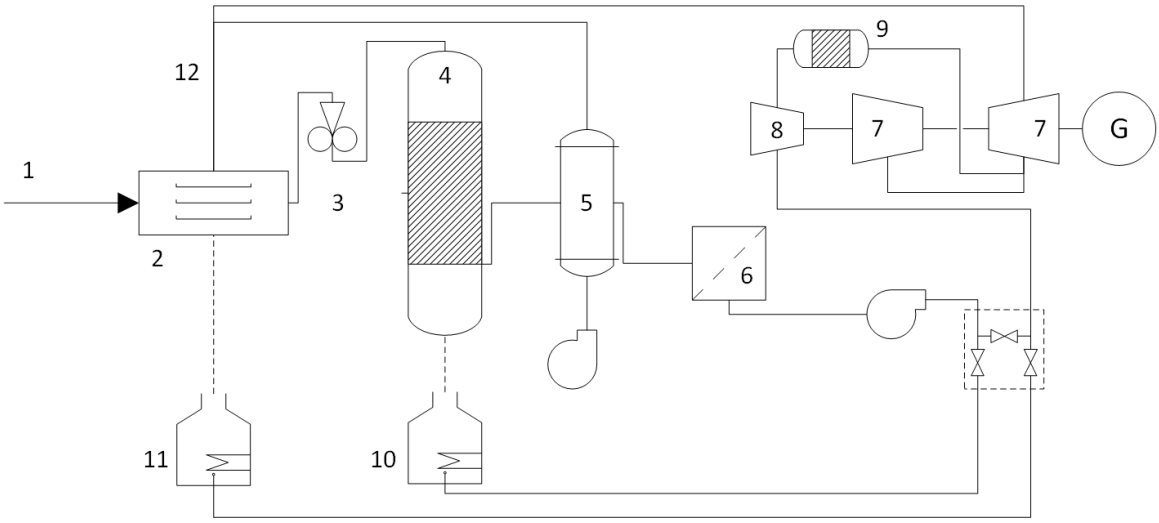

Figure 2.4: Gas turbine system flowsheet. 1: sludge feed, 2: dryer, 3: briquetter, 4: gasifier, 5: syngas HX, 6: filter, 7: gas turbine, 8: fuel compressor, 9: combustor, 10: dryer heating burner, 11: gasifier heating burner, 12: recycled gas streams.

natural gas fired dryer. The centrifuge described in Section 2.2 would likely be required by the thermal drying process [4] to reduce dryer size and cost. Thus, the base case is composed of a centrifuge, wet sludge conveyance equipment, and a natural gas fired dryer. This choice represents a probable sludge management scheme in urban wastewater treatment. Recall that odor and footprint concerns restrict the ability of small urban WWTPs to stabilize sludge by digestion or solar drying. Both the gasifier plant and thermal dryer are expected to operate at 90 % uptime.

Calculation of PW begins with net annual cash flow, F_n, which is the difference between the annual cash flows of the gasification plant and the base case.

$$F_n = [(R_{\text{elec}} + R_{\text{fuel}}) - (C_{\text{capital}} + C_{\text{mfg}})]_{\text{gasification}} - [(C_{\text{capital}} + C_{\text{mfg}})]_{\text{base case}} \tag{2.15}$$

where R is a positive valued revenue, C a negative valued cost, *elec* is electricity revenues, $fuel$ is natural gas cost, *capital* is the cost of financing, and mfg is manufacturing costs. Annual capital costs are determined by adding the cost of capital to the project's installed cost, the total capital investment (TCI), and dividing by the operating life of the plant in k

years.

$$C_{capital} = \frac{TCI(1+r)^n}{k} \tag{2.16}$$

Rate n is the cost of capital, such as a bond rate or mortgage rate and n is the number of compounding periods. As the gasification plant consumes negligible variable cost (no supplemental fuel, etc.) its costs are considered to be only capital investment and finance charges as given in Equation 2.15. Gasification plant revenues are savings from on-site power generation and relieved dryer fuel costs. As the base case produces no value-added products its annual cash flow is simply its costs. Capital investment and finance charges for the drying equipment are assumed to be identical for both cases. Thus the capital costs of the drying equipment cancel from both terms in Equation 2.15 and the cash flow of the base case is simply the purchase price of natural gas. On an annual compounding basis, the present worth, PW, of a project is given by [88]

$$PW = \sum_{n=1}^{N} F_n(1+r)^n \tag{2.17}$$

for a project evaluated every year n for N years. Plant operating life is expected to be 20 years. Variable r represents the minimum acceptable rate of return (MARR). Publicly owned treatment works are expected to be financed solely through municipal debt and are not expected to generate net profit. Thus, MARR is initially estimated to be equal to a representative municipal bond rate. According to the U.S. Federal Reserve [89], a mean average of 20-year AA rated United States municipal bond rates from 2000-2012 is 4.62 %. However to account for unforeseen contingency costs the analysis takes a conservative approach; MARR is set to 10 % [18].

Cost estimation proceeds according to the percentage of delivered equipment costing method. This method assumes the total cost of building and commissioning a plant is a function of the total purchased equipment cost (TPEC). Purchased equipment is taken to mean major process equipment items such as the gasifier, dryer, engine-generator, etc. TPEC is multiplied by a number of empirically determined factors to estimate direct and indirect

costs and working capital. Cost factor method estimates are typically accurate to +/- 30 % [88]. Direct costs are equipment installation, construction supplies, and other hardware and construction related costs. TPEC is included in direct costs. Indirect costs account for engineering, supervision, contingency costs, and construction expenses such as tools and temporary facilities, etc. Contingency costs in process plant construction represent funds set aside for any unexpected cost during plant construction and commissioning. Working capital accounts for capital held in the production process including raw and finished material in stock, cash on hand, and other business related capital. Cost factors used in this analysis are shown in Table 2.1. These costs are summed according to Equation 2.18 to determine total capital investment.

$$TCI = C_{\text{direct}} + C_{\text{indirect}} + C_{\text{working}} \tag{2.18}$$

The cost factors in the Peters and Timmerhaus text [88] are generally calibrated to larger process systems which may require yard improvements and utility service installation. These factors are modified to reflect the likely costs of a small generating plant (Table 2.1). First, operation of the gasification plant and the base case both hold no saleable raw material or product in inventory. Inventory is restricted to maintenance goods including lubricants and spare parts. A low working capital factor of 5% is assumed. Operating costs can be interpreted as business overhead. Such costs are labor, supervision, insurance, taxes, and others. In the context of a wastewater treatment plant, non-labor costs are regarded as a small fraction of the operating costs of the overall wastewater treatment utility. It is assumed that the gasification plant will contribute negligible non-labor overhead to that already accounted for in the base-case. Commercial experience [59] suggests maintenance of an n^{th} plant gasifier system may demand less than eight hours per day of operations and maintenance labor. Labor cost is found by assuming eight hours of operator labor per day during plant uptime where labor cost is found from [90]. Supervision cost is found by multiplying the appropriate cost factor by labor cost. It is expected that a gasification plant will occupy the same building facilities needed by a thermal stabilization system. Thus,

only limited additional construction is necessary, reflected in the small building and yard improvement cost factors. Finally, municipal treatment works in the U.S. are commonly considered tax exempt. Taxes and tax savings from depreciating capital equipment are neglected.

Table 2.1: Cost factors used in the gasifier plant cost model [88].

Direct Costs	**Cost Factor**	**Fixed Operating Costs**	**Cost Factor**
Installation	0.2	Maintenance	0.2
I&C	0.26	Laboratory	0.05
Piping	0.2	Supervision	0.15*Labor
Electrical	0.2	Overhead	0.25*(Labor+ Maintenance+Supervision)
Buildings	0.1	Insurance	0.0125
Yard Improvement	0	Taxes	0
Service Facilities	0	General Expenses	0.05
Indirect Costs	**Cost Factors**		
Engineering	0.03		
Construction	0.01		
Legal	0.01		
Contractor's Fee	0.19		
Contingency	0.37		
Working Capital	0.05		

Major equipment costs for all components except the gasifier were determined from literature sources [91] and supplier quotations. Costing a small-scale downdraft gasifier is challenging; little literature exists on the techno-economics of small-scale biomass power. The literature found to date is vague in regards to component costing, perhaps reflecting limited industrial experience with small scale TCC. No definite costs could be found for the

gasifier. Gasifier cost was estimated from a large scale atmospheric fluidized bed reactor [91]. A fluidized bed reactor is more expensive than a downdraft reactor, making this substitution conservative. Costs are scaled by capacity via Equation 2.19 [42], where C_{new} is the scaled cost, C_0 is quoted cost, Capacity_0 is the quoted capacity and Capacity_{new} is the capacity the cost is scaled to,

$$C_{new} = C_0(\frac{\text{Capacity}_{new}}{\text{Capacity}_0})^{0.6} \tag{2.19}$$

Finally, the costs of electricity and natural gas are sourced from the United States Energy Information Administration under the assumption that electrical power is charged at the industrial rate [92, 93].

Where costs are obtained in a year different than analysis year 2010, Equation 2.20 is used to adjust costs to United States Dollar inflation

$$C_{2010} = C_t(1+d)^{(2010-t)} \tag{2.20}$$

where C is cost, t is any year, and d is the inflation rate [94].

CHAPTER 3

RESULTS AND DISCUSSION

The gasifier model is semi-empirical and must be calibrated such that gas composition and η_c match experimental data. Five variables are specified in the model: temperature, pressure, fuel moisture, η_c, and $T_{\text{equilibrium}}$.

Examination of the literature data shows that gas composition and η_c are strong functions of temperature when the molar carbon to oxygen ratio of the fuel is less than unity, C/O $\leq$ 1. An operating condition of C/O $\leq$ 1 indicates sufficient oxygen is present to gasify solid carbon under Reactions 1.1a-1.1g. In the directly heated air process, sufficient oxygen is also present for partial combustion. Little experimental data exist, especially for steam gasification, at C/O >1. Hence the model gasifiers are planned to operate at or near C/O = 1 which is generally regarded as providing the greatest syngas LHV [52].

Carbon conversion efficiency, η_c, is a function of various parameters including temperature, pressure, fuel moisture, fuel composition, reactor design, and other factors. The data of [28, 56, 95, 96] show a roughly linear increase in η_c with temperature up to about 850 °C where further increase in temperature does not increase η_c. A much smaller effect was observed with molar C/O ratio. Thus, under the condition that molar C/O $\leq$ 1, η_c has been simplified to depend only on temperature. Nonetheless, η_c data used in the model were taken from experimental data points with ER or C/O ratio closest to the value in the simulation. Data used in the model are reported in Table 3.1. This simplification allowed a linear curve to be fit to experimental η_c data, automatically specifying η_c in the model at each temperature point. The simplification allowed gas composition to be dependent on $T_{\text{equilibrium}}$ only, since all other variables were specified from the experimental literature. Error in functionalizing η_c and gas composition as purely temperature dependent is less than 3 % [56] for wet fuel. The temperature dependence simplification reduces the degrees of freedom available to the

gasifier to three, $T_{\text{equilibrium}}$ for Reactions 2.9-2.11, all of which are equilibrium temperatures. Gasifier chemistry was calibrated to fit the literature data by varying $\Delta T_{\text{approach}}$ for reactions 2.9-2.11 until model gas predictions converged to experimental data over the temperature range of interest (700 °C-1000°C). The chemical composition of the experimental sludge was used for calibrations (see Table 3.3).

Table 3.1: Dependence of carbon conversion efficiency, η_c, on gasification temperature

Temperature	η_c Air Process	η_c Steam Process
700	60 %	70 %
750	75 %	75 %
800	80 %	85 %
850	88 %	93 %

3.1 Gasifier Calibration and Validation

Sludge gasification is generally investigated in the temperature range of about 650 °C to 1100 °C. It is expected that temperatures less than 700 °C will lead to incomplete gasification while temperatures in excess of 1100 °C risk ash agglomeration [97] and an increase in heavy metals entrained in the syngas stream [66]. The experimental wastewater sludge gasification literature [56, 79, 95, 96] give η_c and gas compositions as functions of temperature, moisture, and, for air blown systems, equivalence ratio. Equivalence ratio is defined on a mass basis as

$$ER = \frac{\text{Fuel/Oxidizer}_{actual}}{\text{Fuel/Oxidizer}_{stoich}} \tag{3.1}$$

For calibration of the air blown process, the energy balance *DesignSpec* described in Section 2.4 is temporarily relaxed and instead ER is set to the literature value. Gasifier heat demands are assumed to be satisfied by an outside heat source in keeping with the externally heated experimental reactors in the works cited above. Approach temperature results are

given in Table 3.2.

Table 3.2: Restricted equilibrium model approach temperatures evaluated for 700 °C-1000 °C using sludge composition in Table 3.3.

Reaction	**Air Process** $\Delta T_{\text{approach}}$	**Steam Process** $\Delta T_{\text{approach}}$
$CO + H_2O \rightleftharpoons CO_2 + H_2$	202 °C	-290 °C
$C + H_2O \rightleftharpoons CO + H_2$	55 °C	0 °C
$C + 2H_2 \rightleftharpoons CH_4$	-55 °C	-45 °C

Gasifier calibration was validated by comparing model gas composition to experimental data at various gasifier temperatures. Validation runs were conducted using the proximate and ultimate analyses of the wastewater sludges in Table 3.3. Of note is the difference in fixed and ultimate carbon composition between the air process study [56] and the steam process study [79] which demonstrates the geographic variability in sludge composition. The air process study was based on urban Spanish sludge while the steam process used Thai sludge. The variability in fixed carbon content can be attributed to both WWTP process design and retention time. This variability suggests that design-basis modeling efforts should be based on laboratory gasification data from WWTP specific sludge.

A sum of error squared method [98] was used to evaluate the simulation results. Relative error (RE) for a set of N data points is defined as

$$RE = \sum_{i=1}^{N} \left(\frac{\chi_{e,i} - \chi_{m,i}}{\chi_{e,i}}\right)^2 \tag{3.2}$$

where e refers to experimental data, m refers to model data, and χ is a mole fraction. Mean relative error is given by $\sqrt{RE/N}$. Model error is reported in Table 3.4.

The air gasification model generally validates well, capturing the trend of gas evolution over the temperature range investigated (Figure 3.1). Experimental data are represented by point markers in the plot. CH_4 shows the highest relative error, 112 %, whereas the

Table 3.3: Chemical characteristics of wastewater sludges used for model validation.

Analysis [wt %]	**Air Process**[1]	**Steam Process**[2]
Fixed Carbon	7.0	21.8
Volatile Matter	53.7	44.3
Ash	41.3	33.91
C	28.7	45.79
H	4.8	2.99
O	19.8	14.7
N	4.5	1.49
S	0.90	1.11

[1] [56] [2] [79]

Table 3.4: Model validation gas composition and LHV error.

Analysis	**Error (Relative %)**	
	Air Process	Steam Process
H_2	15.1	9.30
CO	23.2	33.0
CO_2	19.5	10.8
CH_4	112	74.8
N_2	3.03	Not reported by experimenter
LHV	6.72	4.35

remaining air process species errors are under 25 %. Thermodynamic equilibrium methods tend to over predict CH_4, yet remain the best modeling choice for interrogating system designs at an early stage [76]. Nonetheless, the air process error is consistent with other ASPEN Plus modeling efforts [98].

The steam process model performance is seen in Figure 3.2. Again CH_4 shows the greatest error over the temperature range, at 74.8 %. CO is in error by 33 % at 700 °C, however the CO curve converges to experimental data by 800 °C, with error not exceeding 7.1 % at gasification temperatures greater than 800 °C. No substantial excursions are seen at other data points. In general, the steam model reproduces the experimental trends well.

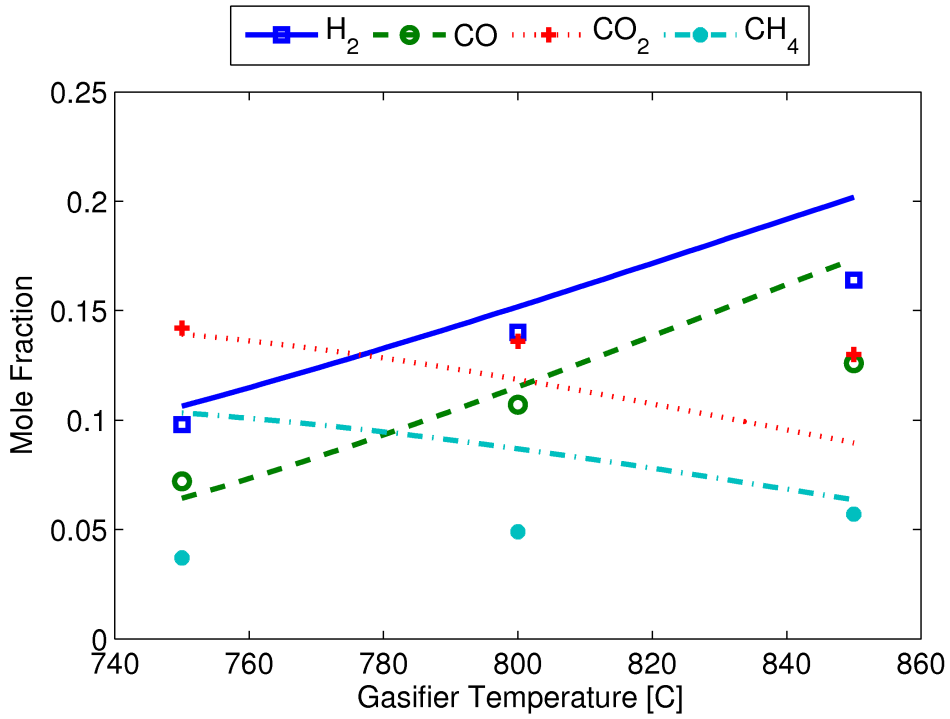

Figure 3.1: Air process validation. Gas composition predicted by the air process model (solid lines) compared to experimental data (markers) for the indicated gasification temperature. Model set to the operating conditions (T,P,η_c, ER) and sludge composition (Table 3.3) of the experimental investigation [56].

In addition to overall composition, calculated syngas LHV was compared to the experimental data. Syngas LHV represents the chemical potential energy of the fuel stream, and is more important to a thermodynamic analysis than gas composition [76]. Despite significant

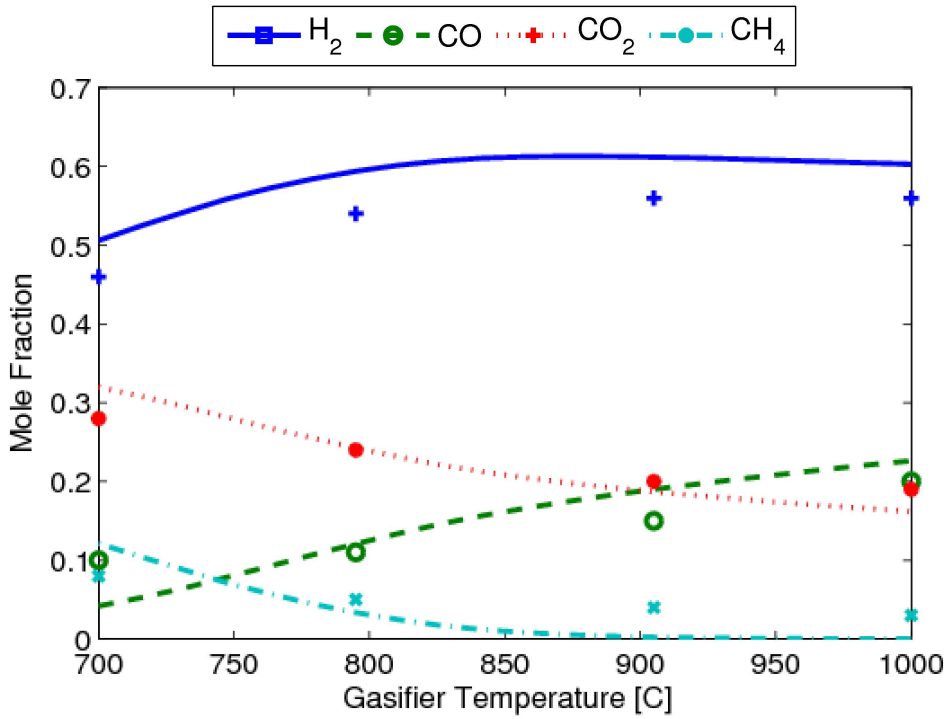

Figure 3.2: Steam process validation. Gas composition predicted by the steam process model (solid lines) compared to experimental data (markers) for the indicated gasification temperature. Model set to the operating conditions (T,P,η_c, mass basis steam/sludge ratio) and sludge composition (Table 3.3) of the experimental investigation [79].

error in gas composition, air process syngas LHV is in error by only 6.7 %. Steam process LHV is in excellent agreement with experiment at 4.3%. From this data it can be taken that the restricted equilibrium model is capable of simulating air and steam blown gasifier chemistry with a degree of accuracy appropriate for a thermodynamic analysis. LHV validation data are presented in Figure 3.3.

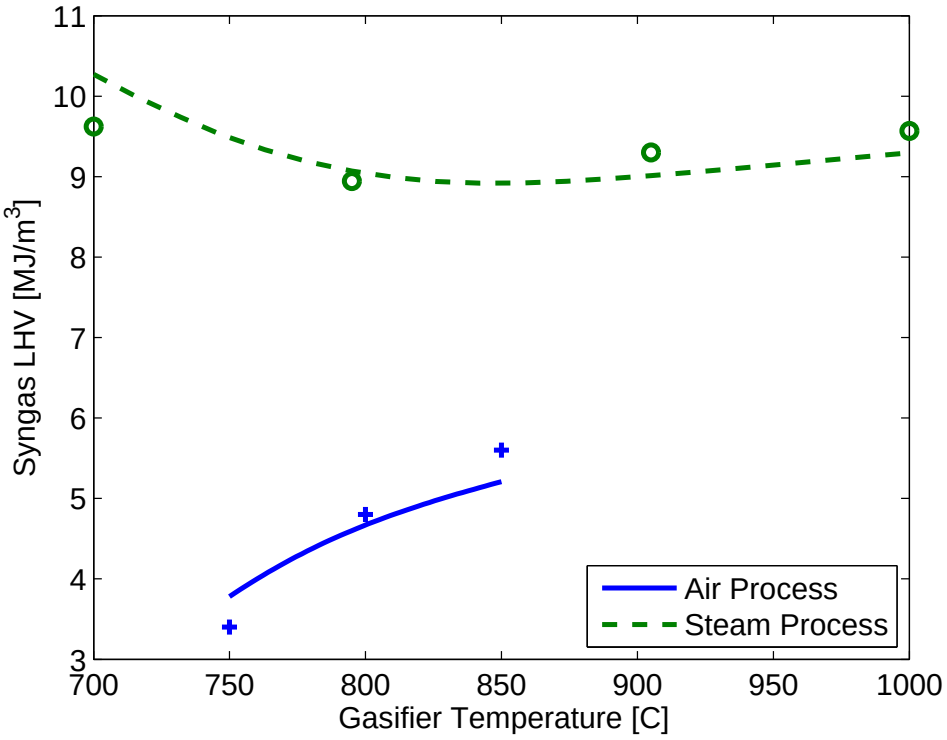

Figure 3.3: Syngas LHV validation. Dry basis volumetric LHV of syngas (including N_2, CO_2) computed by the model compared to experimental data at the given temperature. Model set to the operating conditions and sludge composition (Table 3.3) of the experimental investigation [56, 79]. LHV calculated as $\sum \chi_i LHV_{\text{molar},i}$

3.2 Optimized Operating Conditions

Optimized thermal system design implies that all degrees of freedom in the system specifications have been investigated. In engineering design, some flexibility is lost by upstream design choices placing limits on other variables. For example, the choice of a spark ignition engine restricts the maximum syngas delivery temperature to relatively low values. While

a high-level thermodynamic analysis such as this cannot possibly consider all design variables, some process thermodynamic variables can be optimized. In particular, this analysis anticipates gasifier temperature and fuel moisture (post-dryer) to have a great impact on electrical output, and therefore, economic feasibility.

Optimizations for all variables were performed through parametric studies maximizing net electrical output. ASPEN Plus offers the ability to optimize an entire system, with numerous variables, against one or more objective functions. An attempt was made to simultaneously optimize the entire system for net electrical output. However, computational stability and numerical solver convergence issues precluded such a solution.

3.2.1 Gasifier

In order to optimize gasifier temperature and fuel moisture, parametric studies were conducted for gasifier temperature between 700 °C and 1000 °C and fuel moisture between 10 wt % and 80 wt %. Simulation results quickly revealed that system energy balance could not be satisfied with fuel moisture in excess of 55 wt %. At moisture concentrations in excess of 55 wt %, total system heating duty increased beyond the fuel energy supplied. Thus fuel moisture was constrained to 10 wt %-55 wt %.

First, fuel moisture concentration was analyzed. The air process admits sufficient oxygen to satisfy the gasification reactions and close the gasifier energy balance by partial combustion. No gains are realized from oxygen introduced with increased fuel moisture. Instead, excess moisture serves to increase the gasifier heat duty and thus the fraction of fuel combusted in the gasifier. Correspondingly the net power curve in Figure 3.4 decreases monotonically with increased fuel moisture. In the region between 10 wt % and 15 wt % moisture, the net power decreases relatively slowly, indicating that this moisture range is a stable operating point. Nonetheless, 10 wt % water is the optimum operating condition to maximize electrical output. This conclusion must be tempered with the understanding that carbon conversion efficiency is functionalized only by temperature dependence; experimental literature [28, 56, 96] suggests that η_c gains (of less than 5 %) are indeed made with increas-

ing fuel moisture. However, the simulation tends to heavily favor dryer fuel. η_c gains may be washed out by reactor heating duty.

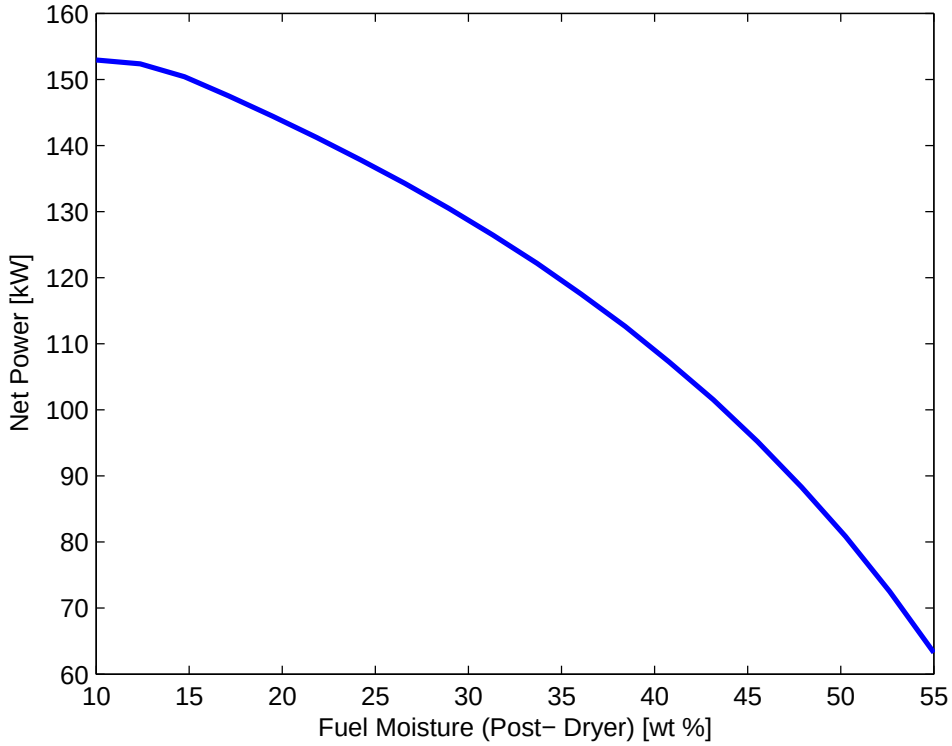

Figure 3.4: Air process moisture optimization. Effect of dried fuel moisture content on net power output of the air process system. $T_{gasifier}$=850 °C. ER calculated dynamically to satisfy gasifier energy balance (see Section 2.4). All other parameters held constant

Steam gasification below ($C/O = 1$) is not seen in the experimental literature. Such conditions are more similar to high-temperature pyrolysis than gasification. Pyrolysis studies [27] provide the best data to approximate the performance of low-moisture steam gasification. Up to 45 % solid matter can remain at 7.1 wt % fuel moisture, suggesting that the temperature dependent carbon conversion approximation used in gasifier modeling breaks down for $C/O > 1$. In the absence of appropriate data to validate the model, steam gasification was explored only between 28 wt % and 55 wt % moisture. In similar fashion to the air process, net power peaks at the lowest possible moisture level (Figure 3.5). This result supports the conclusion that reactor heating duty drives energy efficiency for the indirectly heated steam process.

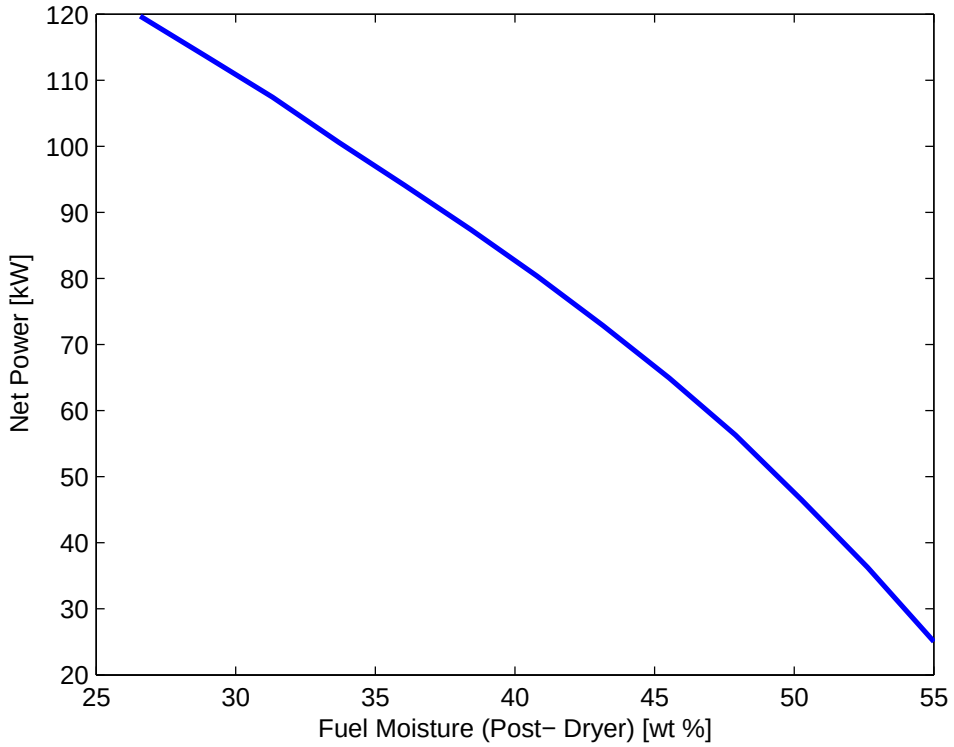

Figure 3.5: Steam process moisture optimization. Effect of dried fuel moisture content on net power output of the steam process system. $T_{gasifier}$=850 °C. Gasifier burner duty calculated dynamically. All other parameters held constant

The results of the moisture analysis do not change in form for any analysis temperature between 700 °C and 1000 °C. Thus the temperature studies were conducted at the optimized moisture concentrations, 10 wt % for the air process and 28 wt % for the steam process. The air process shows a curious response to temperature, seen in Figure 3.6. Net power output is nearly zero until about 750 °C. Two phenomena can explain this effect. First, η_c of the air process at 700 °C can be as low as, 55 % [56]. At these low temperatures a great quantity of fuel energy is wasted as char. A more detailed treatment of the effect of η_c on net power output is presented in Section 3.6. Second, process energy efficiency is heavily influenced by heat and mass flow from the syngas cooler. At low gasification temperatures insufficient heat is transferred from the syngas into the dryer. All of the produced syngas must be diverted to the dryer burner. At 850 °C and above, η_c attains its maximum value of 88 %. Increasing temperature further demands more sludge must be burned to satisfy heating loads and no electrical output gains are realized.

The steam process begins with higher η_c, 70 % at 700 °C and thus is able to produce net electrical power at low temperatures, although the energy efficiency is poor. The steam process response to temperature is shown in Figure 3.7. Here again the gain in net power output between 700 °C and 850 °C is due to the combined effects of increasing η_c and increasing heat transfer from the hot syngas to the dryer. The much sharper decline in net electrical power at temperatures in excess of 850 °C is due to low efficiency external heating. Considering these results the air blown system is specified at 850 °C and 10 wt % moisture and the steam blown system is specified at 850 °C and 28 wt % moisture.

Syngas composition at the net power optimized operating conditions is reported in Table 3.5. As expected, the air process syngas is substantially diluted by atmospheric N_2 due to the need to admit 34 % of stoichiometric air for partial combustion. These data are generally similar to the results of laboratory-scale sludge gasification performed by De Andrés [56] and Manyá [96]. Air process LHV of 4 MJ/kg is near the minimum value for stable combustion in spark-ignition engines [83]. Combustion stability may be improved by increasing the mole

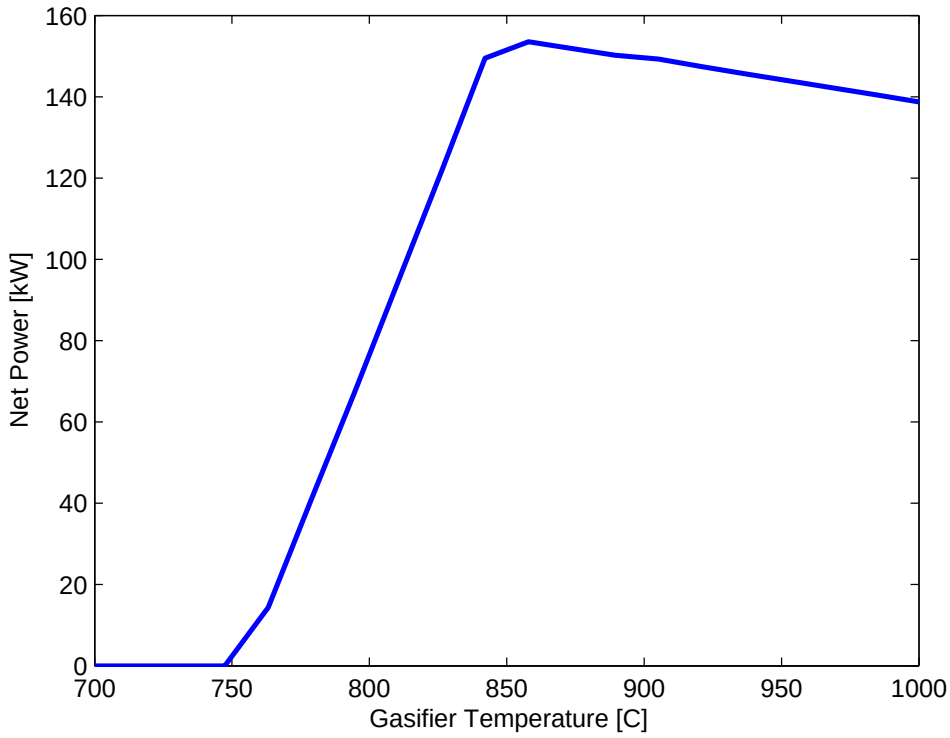

Figure 3.6: Air process temperature optimization. Effect of gasification temperature on net power output of the air process system. Fuel moisture held constant at 10 wt %, ER calculated dynamically. All other parameters including equilibrium approach temperatures (Table 3.2) held constant.

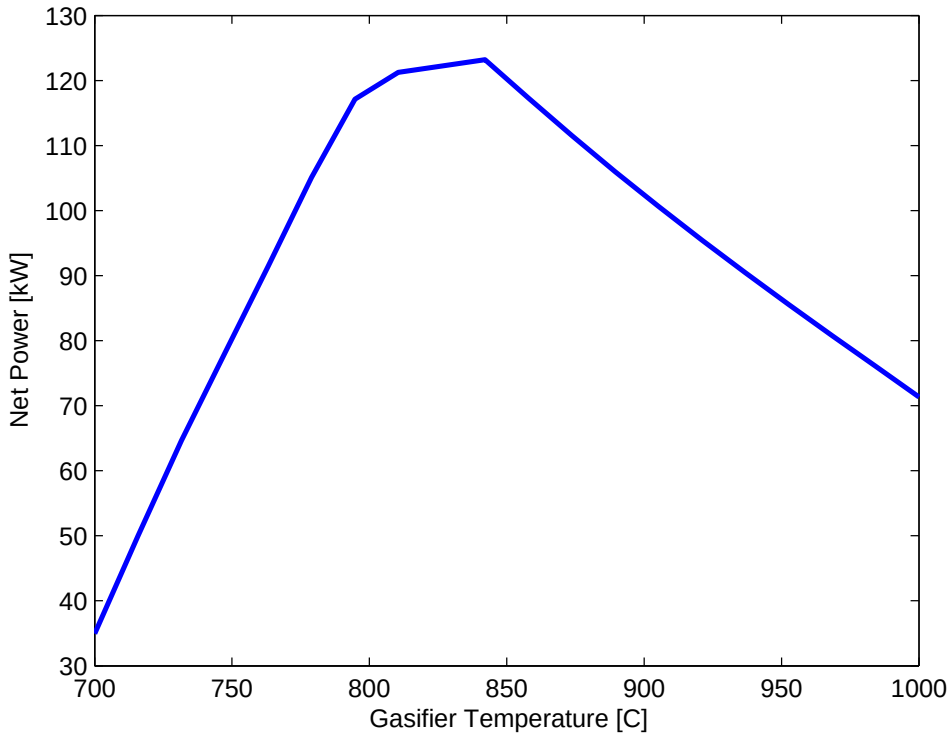

Figure 3.7: Steam process temperature optimization. Effect of gasification temperature on net power output of the steam process system. Fuel moisture held constant at 10 wt %, gasifier heating burner duty calculated dynamically. All other parameters including equilibrium approach temperatures (Table 3.2) held constant.

fraction of H_2 [84]. H_2 concentration can be increased in-situ by steam reforming CH_4 and water-gas shifting CO through the reactions 1.1f and 1.1g by admitting more water with the fuel. Since the air process fuel moisture optimization suggests little power decrement occurs when increasing from 10 wt % fuel moisture to 15 wt % fuel moisture, this approach may be successful. Indeed, increasing fuel moisture to 15 % results in the mole fraction of hydrogen increasing by about 5 %. Net power is decreased by only 4.5 %. Whether in-situ steam reforming is necessary depends greatly on the engine used in a real system. High compression engines, engines with multiple spark plugs, and combustion chamber designs which promote efficient mixing and high turbulent flame speeds may operate successfully on the low LHV gas without any reduction in net power.

In comparison to the air process, steam process syngas appears substantially more valuable, with H_2 concentration approaching 50 % due to little dilution by non-reactive species. The high moisture content, 28 wt % water, promotes substantial in-situ steam reforming. However the greatest reason for the high concentrations of fuel species is the lack of N_2 dilution.

Table 3.5: Simulated synthesis gas composition

Analysis	**Mole percent Air Process**	**Mole percent Steam Process**
H_2	15.1	49.1
CO	17.8	29.7
CO_2	7.0	7.4
CH_4	1.2	7.0
H_2O	11.2	3.6
N_2	47.7	2.7
LHV [MJ/kg]	4.0	17.0

3.2.2 Syngas Cooler

A further optimization study was conducted to determine syngas cooling temperature. As described in Section, 2.5, the syngas cooling heat exchanger is specified for cooled syngas temperature, hot air outlet temperature, and temperature approach. A *DesignSpec* block determines the mass flow of air needed to satisfy the specifications. To investigate the system response to syngas cooling conditions, hot air outlet temperature was varied between 120 °C and 830 °C. These temperature bounds were selected as the lowest temperature where tars remain in vapor phase is about 120 °C [58], and 830 °C accounts for temperatures losses between the 850 °C gasifier and the heat exchanger. The lower temperature bound drives the greatest mass flow of air and may allow for low temperature (and high efficiency) drying. Evaporation at low temperature is driven by suppressed equilibrium. The partial pressure of water vapor in the drying gas may be forced far below the equilibrium concentration at a given temperature due to the high mass flow, driving mass transfer to the vapor phase. Thus, the dryer may operate at temperatures lower than 100 °C. The upper temperature limit obviously requires a counterflow heat exchanger design and will create a very low mass flow of cooling air.

Simulation results from both processes show net power peaks at a cooling air exit temperature of 300 °C. However the sensitivity is fairly low for any outlet temperature. Net power decreases by only 6 % at either temperature bound.

3.3 Thermal Performance

The effectiveness of waste heat recovery is demonstrated by comparing the energy requirement to dry sludge as a function of moisture content with and without heat recovery. Sludge is assumed to enter the system at 80 wt % initial moisture from an upstream centrifuge. Figure 3.8 shows the effect of heat recovery. The solid line is dryer heat demand with no heat recovery, the dashed line is the air process, and the dotted line is the steam process. The no heat recovery curve shows the mass specific energy needed to evaporate

water from sludge as simply Δh_{fg} normalized to sludge infeed energy as

$$\frac{\Delta h_{fg}}{\dot{m}_{sludge} LHV_{sludge}} \tag{3.3}$$

The heat recovery curves show energy needed in excess of recovered heat in the modeled convective dryer computed as

$$\frac{\Delta h_{fg} - \dot{Q}_{recovered}}{\dot{m}_{sludge} LHV_{sludge}} \tag{3.4}$$

where $\dot{Q}_{recovered}$ is the total heat recycled to the dryer. Note that negative dryer heating duty is manifested as a dryer exhaust temperature above dew point (see Section 2.3).

Waste heat recovery reduces net dryer heating demand substantially. Both air and steam processes demand no additional drying energy in excess of that supplied by the syngas heat exchanger and engine exhaust for outlet moisture of 15 wt % or greater. At 10 wt % moisture, the air process demands about 2 % of the produced syngas to fuel a burner to provide auxiliary drying heat. Examining dryer heating duty at various gasification temperatures provides insight into the system's thermal integration. Figure 3.9a shows the variation in dryer heating duty for various gasifier temperatures for the air process. Figure 3.9b shows similar data for the steam process. In both cases, dryer heating duty reduces dramatically between 750 °C and 1000 °C. High temperature syngas gives up most of its sensible heat to cooling air in the syngas cooling heat exchanger. As the syngas outlet temperature is specified at 150 °C, increasing gasifier outlet temperature serves to increase the mass flow rate of cooling air. The expected result of flowing larger mass flows of hot air into a dryer is to reduce the amount of excess energy required by the drying process. As gasifier temperature approaches 1000 °C, mass flow of hot air to the dryer more than satisfies drying load. These results, while perhaps not immediately practical for the optimized gasifier temperature of 850 °C, prove that effective dryer thermal integration is indeed possible.

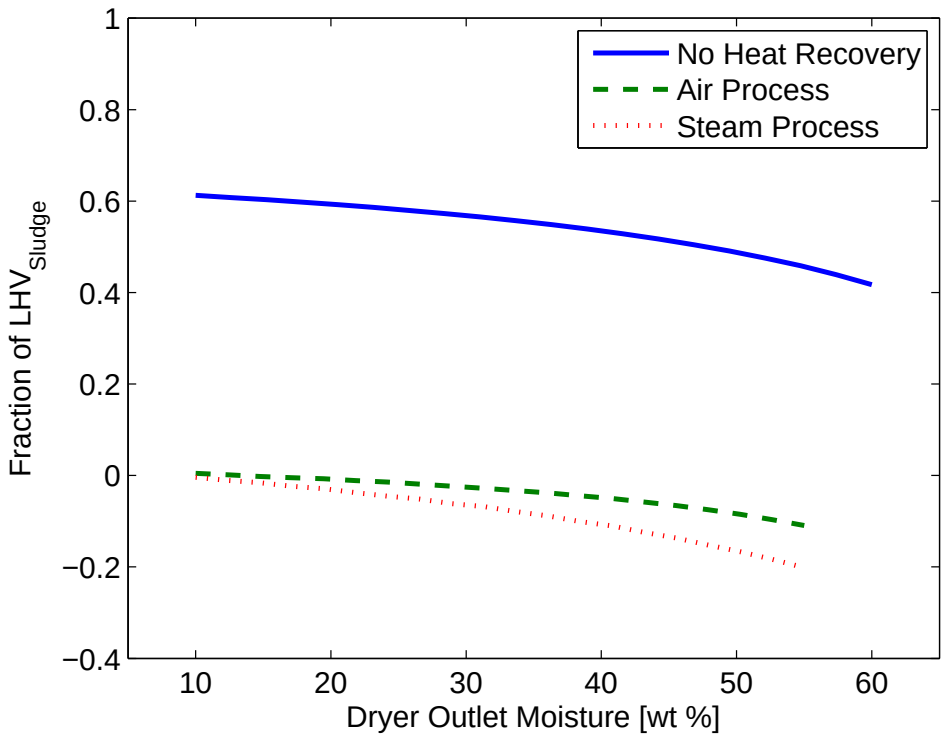

Figure 3.8: Thermal performance of the air and steam processes. Plot shows the energy needed to dry sludge in addition to recycled heat streams. The energy needed to dry without any heat recovery is shown for comparison as Δh_{fg}. Negative drying energy represents a dryer outlet temperature $T > T_{\text{dew point}}$. The ordinate scale is normalized to display drying energy requirements as a function of $\text{LHV}_{\text{sludge}}$.

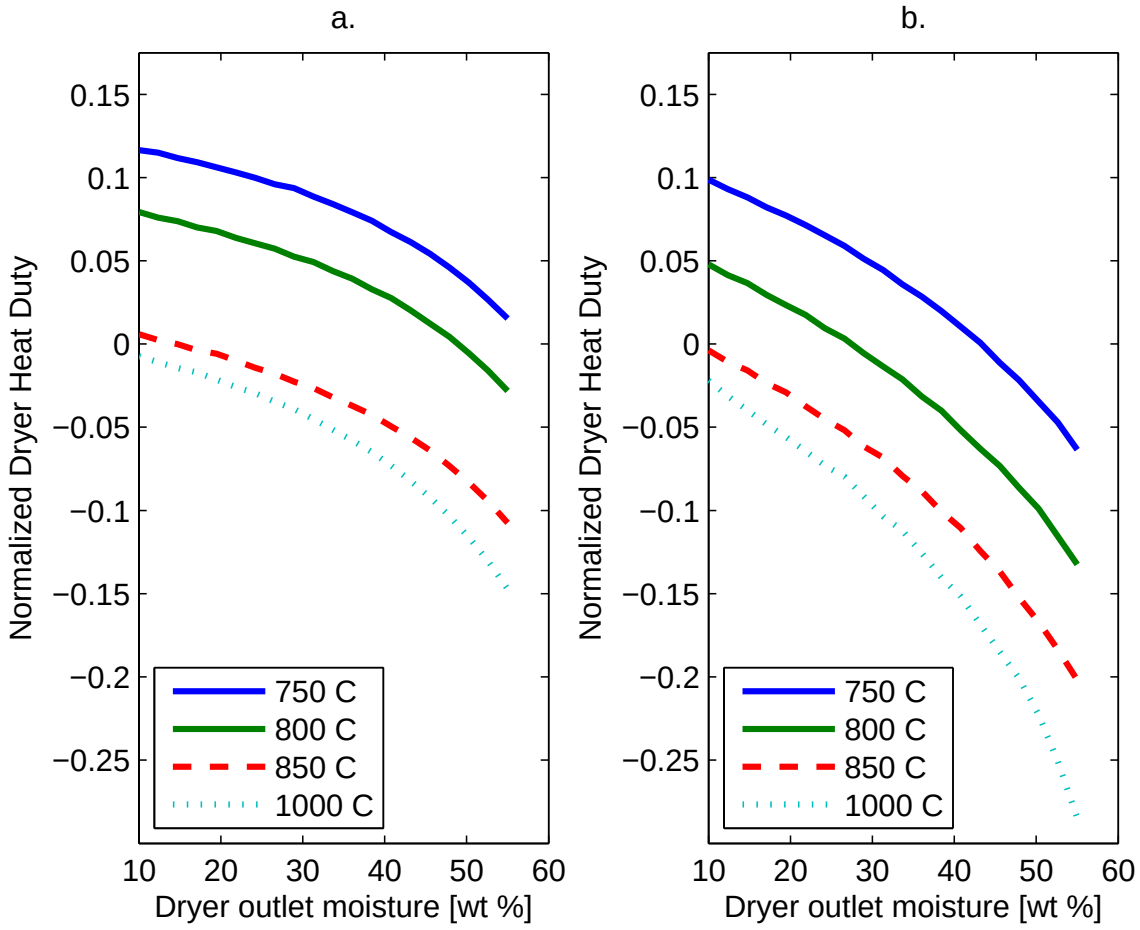

Figure 3.9: Dryer heating duty as a function of outlet moisture at various gasifier temperatures. Data demonstrate the effect of recycling heat from syngas cooling to satisfy drying loads. Higher gasifier temperatures allow more energy to be recycled to the dryer via the syngas cooler; less energy is needed from the auxiliary burner. Negative drying energy represents a dryer outlet temperature $T > T_{\text{dew point}}$.The ordinate scale is normalized to display drying energy requirements as a function of LHV_{sludge}.

3.4 Electrical Performance

Net electrical output of both the air process and steam process models are presented in Figure 3.10 as a function of fueling rate. The solid line represents the air process, the dashed line represents the steam process. Data points are the net power output of commercially available small scale biomass gasification systems, [59, 99].

Both the air and steam systems show a linear relationship between fueling rate and net power output. Since the model assumes all components are designed for the material and energy flow rates at any point, this is an expected result. The air process is seen to outperform the steam process by about 26 %. A 26 % difference is larger than the mean relative error between model and experimental syngas LHV, suggesting that this conclusion is robust. In terms of specific electrical output the air system delivers 0.788 [kWh/kg] and the steam system 0.456 [kWh/kg].

The large difference in net power output is explained by process energy demands; specifically the heat duties of the dryer and gasifier. Gasifier heating for the air process is satisfied by admitting molecular oxygen in excess of that needed to fully gasify all fuel carbon. Excess oxygen drives Reactions 1.1a-1.1b further toward products, releasing sufficient heat to satisfy reactor heat demand. Simulation results show a calculated equivalence ratio of 34%, meaning that 34 % of the initial fuel sludge is burned to heat the gasifier to 850 °C. In contrast, the steam process burns about 56 % of the product syngas, or 67.2 % of the initial fuel sludge, to heat the gasifier. Two phenomena explain the greater heat duty of the steam process. First, the steam process is heating an additional 18 wt % more water than the air process. Second, heat must be transferred from an external source, in this case a burner and heat exchanger. Considering burner heating efficiency to be

$$\eta_{\text{burner}} = \frac{\dot{Q}_{\text{burner}}}{\dot{m}_{\text{syngas}} LHV_{\text{syngas}}} \tag{3.5}$$

where $\dot{Q}_{\text{burner}}$ is the heat transferred from hot combustion gases to the gasfier and $\dot{m}_{\text{syngas}}$ refers to the mass flow of syngas diverted to the burner. Heating the gasifier with a syngas

burner is less than 55 % efficient itself, as heat transfer with the reactor at 850 °C yields an exhaust stream of temperature greater than 850 °C. Nonetheless, a 55 % efficient burner is still about double that of the 27 % efficient engine-generator. Thus electrically powered heating methods were not considered for the steam process.

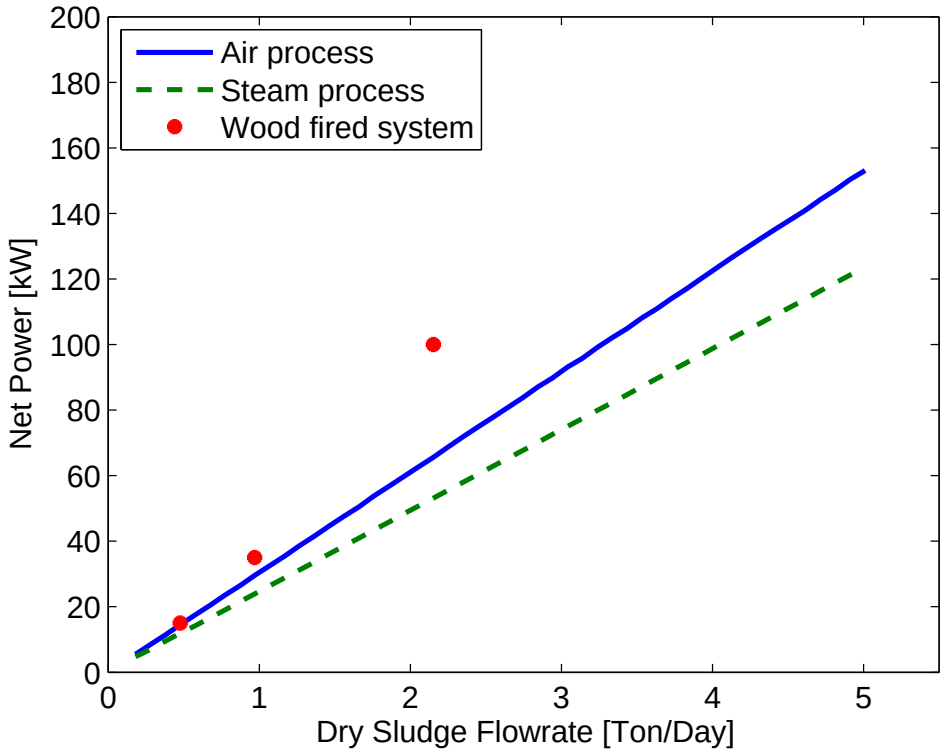

Figure 3.10: System electrical performance. Net electrical power output of the air and steam processes as a function of dry sludge flow rate. System operating conditions are as specified in Section 3.2. Data points are the net electrical output of commercially available wood fired gasifier systems.

The commercial system data points are included to benchmark this sludge fired system against wood fired small gasification energy platforms. Wood fuels carry about 12 % more energy as LHV_{fuel} and 90 % less ash per unit mass than the sludge used in this study [100], suggesting that wood fueled systems will provide greater net power. In addition to the heating value difference, less energy must be expended drying wood to about 10 wt % moisture. The reduced drying load will likely result in lower optimized gasifier temperatures. For example, maximum net electrical output of the modeled sludge fired air process occurs

at a gasification temperature of 850 °C. The wood gasifier system operates at an ash grate temperature of 760 °C [59]. Overall, a wood fired system would be expected to produce greater electrical power than a sludge fired system of similar design. Indeed, simulation bears this out. The net power output of the sludge-fueled system at a fueling rate of 2.2 dry metric ton/ day is 65 kW compared to the 100 kW produced by the wood-fueled system. Given the thermodynamic advantages of wood fuel over sewage sludge the 35 % difference between the systems is not surprising.

Simulation predicts dryer exhaust temperature to be about 70 °C. Such a low temperature precludes exporting useful heat out of the system boundary for most practical applications.

Cold gas efficiency, (CGE), defined as

$$\mathrm{CGE} = \frac{\dot{m}_{\mathrm{syngas}} LHV_{\mathrm{syngas}}}{\dot{m}_{\mathrm{fuel}} LHV_{\mathrm{fuel}}} \tag{3.6}$$

is a figure of merit which relates the ability of the gasifier to convert the chemical energy of the fuel to chemical energy in the syngas. As air blown gasification introduces a nitrogen diluent which reduces the mass basis LHV of syngas, it is sensible that the air process CGE of 71 % is less than that of the steam process, 88 %. Overall system efficiencies are 17.5 % for the air process and 12.3 % for the steam process. Syngas LHV was found to be 4 MJ/kg for the air process and 17 MJ/kg for the steam process. Modeling data confirm that, from a systems perspective, the air blown system is substantially superior.

Major system performance indicators are presented in Table 3.6. System efficiency, η_{system}, is calculated as $\dot{W}_{\mathrm{elec}}/\dot{m}_{\mathrm{sludge}} LHV_{\mathrm{sludge}}$ and engine efficiency, η_{engine}, is calculated as $\dot{W}_{\mathrm{shaft}}/\dot{m}_{\mathrm{syngas}} LHV_{\mathrm{syngas}}$ where the *syngas* subscript refers to gas delivered to the engine. In terms of energy balance closure, the overall efficiency of the system, η_{system} can be compared to the product $\eta_{\mathrm{engine}} * \mathrm{CGE} * \delta$ where δ is the fraction of gas delivered to burners. For both systems the relative difference between calculated system efficiency and the product $\eta_{\mathrm{engine}} * \mathrm{CGE} * \delta$ is less than 5 %.

Table 3.6: System performance indicators.

Indicator	Air Process	Steam Process
Max. Net Power (kW) (5.5 MGD)	153.0	123.7
η_{system} (%)	17.5	12.3
η_{engine} (%)	24	27
CGE (%)	72	88
LHV_{syngas} (MJ/kg)	4.0	17.0
ER (Air process) (%)	34	N/A
Burner Gas (%)	2 (Dryer)	54.2 (Gasifier)

3.5 Combustion Turbine Option

As described in Chapter 2, a spark ignition engine was selected *a priori*, as it was expected to deliver greater overall efficiency and cost effectiveness than a combustion turbine. To test the conclusion, a combustion turbine based model was also investigated. The potential advantage of substituting a combustion turbine for the spark ignition engine is mostly related to a turbine's ability to accept a high temperature fuel stream. Thermodynamic advantage may be realized by recovering the sensible energy of the high temperature syngas in the prime mover instead of recycling the energy directly to the dryer through the syngas cooler (block 5 in Figure 2.2).

The turbine based model was investigated for syngas temperatures of 150 °C and 850 °C. The low temperature 150 °C case is meant to be a comparison to the spark ignition engine model. In similar fashion to the engine model, most of the sensible energy in the hot raw syngas stream is exchanged with cooling air and recycled to the dryer. The high temperature 850 °C case is intended to explore the potential thermodynamic advantage of fueling a combustion turbine with high temperature syngas. The syngas cooler is bypassed completely in this case. In order to ensure maximum performance of the combustion turbine system, a net power optimization for gasifier temperature and fuel moisture was conducted

in similar fashion to the process described in Section 3.2. Perhaps not surprisingly, gasifier operating temperature and fuel moisture conditions which maximize electrical output were found to be identical to the spark ignition system. Gasifier temperatures were 850 °C for both air and steam processes. Fuel moisture was 10 wt % for the air process and 28 wt % for the steam process.

Overall performance of the combustion turbine based systems was found to be inferior to the spark ignition engine based systems. Table 3.7 shows the net power for various syngas temperatures. The turbine based system underperforms the spark-ignition engine based system by about 12 %, delivering 20 kW less shaft power at a sludge fueling rate of 5 dry ton/day. Some interesting trends are evident from the simulation data. Contrary to expectation, net power drops as fuel temperature is increased. Examination of the simulated compressor work streams reveals that fuel compression loads drive the trend. Fuel compressor power is given in Table 3.8. The result is easily explained by considering that syngas specific volume increases with temperature; energy required to compress the gas similarly increases. A similar effect would certainly be seen fueling a reciprocating engine with hot fuel, perhaps to an even greater degree. Hot fueling a reciprocating engine would have the additional effect of greatly reducing volumetric efficiency. However, autoignition concerns render the point moot; spark ignition engines have a limited intake temperature range, generally below 100 °C for hydrogen rich fuels [84].

This effect of fuel compression energy is especially important for low LHV gaseous fuels. The turbine is forced to compress a relatively great mass flow of fuel compared to the turbine's power output. Mass flow of syngas for air process is 0.174 kg/s, compared to only 0.0316 kg/s of steam process syngas. Making a simple comparison with natural gas, taken to be about 50 MJ/kg [68] compared to 4 MJ/kg for air process syngas, a natural gas fired turbine would flow only 0.0139 kg/s for a shaft power of 150 kW. Overall, the combustion turbine system results support the assumption used in the initial project scope that a reciprocating engine will outperform a combustion turbine in small scale applications. Such results suggest

that an indirectly heated gas turbine, using an atmospheric pressure combustor and heat exchanger, may be more efficient. However potential low burner efficiency, Equation 3.5, could reduce any thermodynamic advantage gained by lower compression load.

An option to relieve some of the parasitic demands of fuel compression is pressurized gasification. However the increased reactor and safety systems costs required to run a pressurized gasifier may be too great for a small scale installation. Pressurized gasification is not treated further in this work.

Table 3.7: Combustion turbine system performance at a fueling rate of 5 dry ton/day.

Syngas Temperature	**Shaft Power, kW Air Process**	**Shaft Power, kW Steam Process**
150 °C	150.1	118.0
500 °C	88.0	100.0
850 °C	20.7	87.8
Spark Ignition Engine	170.0	137.4

Table 3.8: Fuel compressor work at a fueling rate of 5 dry ton/day for various fuel temperatures.

Syngas Temperature	**Fuel Compressor Work, kW Air Process**	**Fuel Compressor Work, kW Steam Process**
150 °C	214.7	102.7
500 °C	315.7	140.7
850 °C	408.0	180.8

3.6 Sensitivity to Fuel Composition

Wastewater treatment sludge is a variable composition fuel. Sludge composition varies with numerous factors. Typically, domestic and agricultural wastewaters will have greater

energy content (due to fats and carbohydrate molecules) than light commercial or industrial wastewater sources. Wastewater treatment plant processes also influence the chemical characteristics of sludge. Any process which allows aerobic, heterotrophic micro-organisms (those micro-organisms which oxidize carbonaceous molecules for energy) to operate on wastewater will reduce energy content of the sludge. Such organisms consume carbon based molecules for metabolic energy, evolving CO_2 to the atmosphere [1]. WWTPs which use long retention microbial treatment processes will generate sludges relatively low in chemical energy. Even the length of sewer pipes can influence sludge energy. Long flow paths allow time for micoorganisms to feed on wastewater molecules, evolving CO_2. Wastewater characteristics can even vary in time through diurnal and annual cycles. The sludge literature [1, 22, 23, 56, 79, 96] shows a wide range of ultimate analyses especially regarding oxygen and ash content. Variation is also seen in the proximate analysis, although the compositional characteristics measured by the proximate analysis (fixed carbon and volatile matter mass percentages) do not influence a thermodynamic analysis. Fixed carbon and volatile matter characteristics are quite likely to influence η_c and reaction kinetics; however this model is not capable of simulating kinetic phenomena.

The viability of a waste to energy project depends on the value recovered from the waste stream. A waste to energy technology may not be energetically or economically viable to all WWTPs. To be viable the technology must be capable of accommodating varying sludge characteristics both from a technical standpoint and from a net power, process economics standpoint. It is expected that net power will vary inversely with ash content and oxygen content. Conversely net power output should vary proportionally to carbon and hydrogen content. Two analyses are presented. Figure 3.11 shows the change in net power output as a function composition. Figure 3.12 shows the sensitivity of the model system to fuel composition. Sensitivity is computed as the numerical partial derivative,

$$\frac{\partial \dot{W}_e}{\partial m} = \frac{\dot{W}_{ei+1} - \dot{W}_{ei}}{m_{i+1} - m_i} \tag{3.7}$$

for $\dot{W}_e$ representing electrical power, m_i a mass fraction of C, H, O, or ash, and i is the index variable. The rationale for including the sensitivity is to determine stable operating regions, where small changes in composition have little effect on system performance. For all the analyses in Figure 3.11 and Figure 3.12 the ratio of all fuel components in the ultimate analyses not being varied are held constant, and are only scaled to accommodate the varied component. The analyses were conducted using the air process system at optimized system conditions and the maximum sludge flow rate studied, 5 dry ton/day (0.058 kg/s). Each component is investigated in the range where it can be found in various fuels, specifically sludge, wood, and low rank coal. The rationale for extending the sensitivity analysis beyond sludge is to investigate whether the air process system may be applicable to other fuels.

Oxygen is expected to have a substantial negative effect on system performance. Fuel oxygen implies that the fuel is partially oxidized and will carry less available chemical energy [68]. Figure 3.11a shows that increasing oxygen has a negative effect on net electrical output. Oxygen concentration between about 10 wt % and 30 wt % shows a gentler slope than the higher concentration regions. Fuels in the lower portion of this range are bituminous and lignite coal which have greater LHV than sludge [4]. Some biomass sources including wood, municipal solid waste heavy in plastics, and fatty food wastes can have oxygen mass fractions less than 20 wt %. Sludge varies generally between 25 wt % and 50 wt % oxygen; sludges exposed to aggressive microbial action show the highest oxygen concentrations. Most of the example sludges seen in works cited by this study have oxygen concentrations in excess of 30 wt %. Such high oxygen sludges may produce less than 2/3 the net electrical output of the relatively high energy density domestic and light commercial sludges used in this analysis [23].

Net power sensitivity to oxygen, Figure 3.11a, is relatively stable at 2-2.5 kWe/wt%$_O$ up to about 30 wt % oxygen. The sharp sensitivity increase from 25 wt % suggests an unstable operating condition where up to 6 kW is lost between 28-30 wt % fuel oxygen. From a stoichiometric perspective, at 25 wt % oxygen the molar H/O ratio is unity, the oxygen is

capable of completely oxidizing all fuel hydrogen.

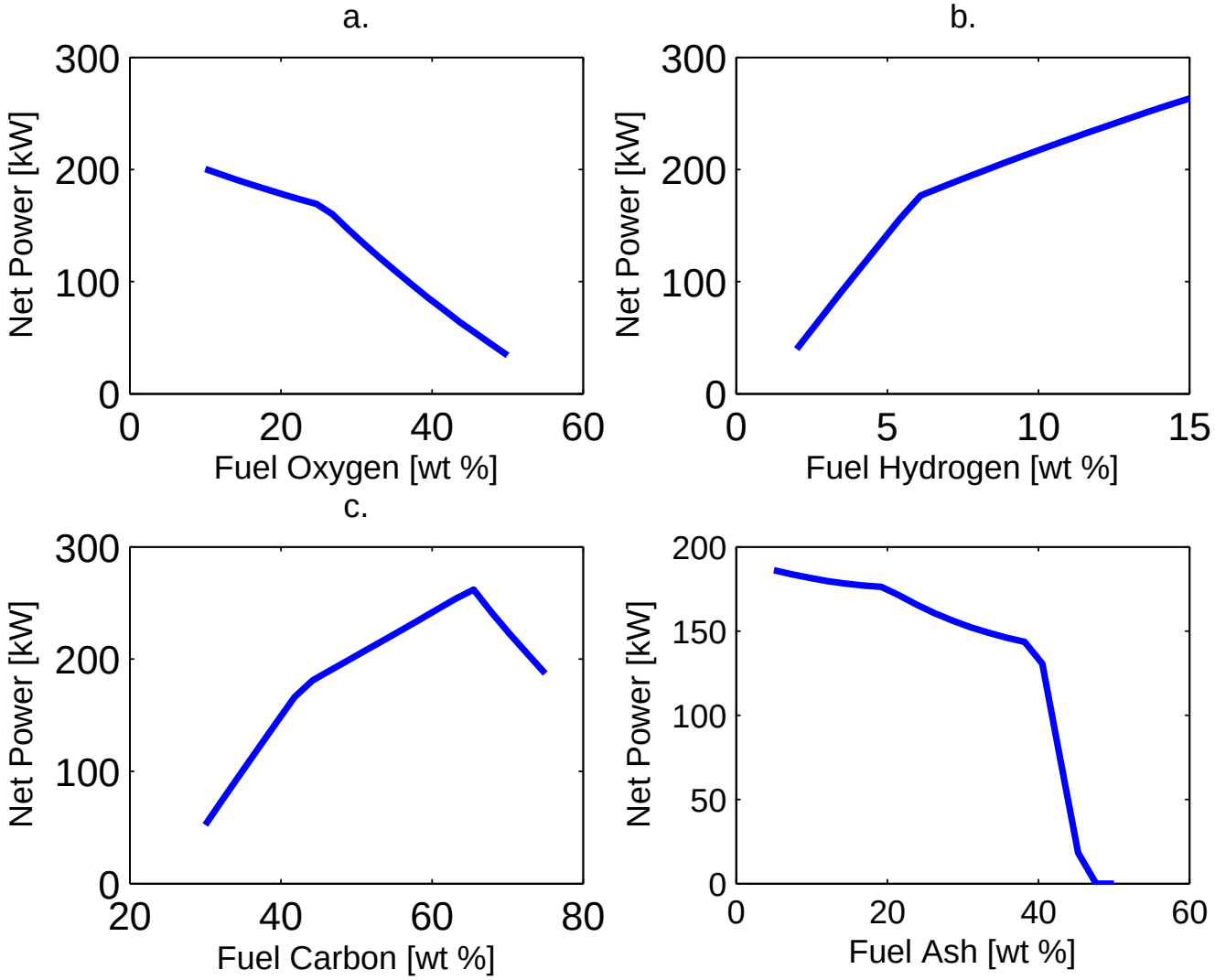

Figure 3.11: Effect of fuel composition on net power output. Fuel composition was varied by adjusting the mass percentage of the selected species while holding the relative amount of all other species constant. Plot a: O_2, b: H_2, c: carbon, d: ash (non-reactive).

As expected, net power output varies proportionally with hydrogen content. Biomass sources usually have a hydrogen mass fraction between 4 and 7 wt % [23, 28–30]. The sensitivity analysis, Figure 3.12b, suggests that net power output is quite sensitive to hydrogen content, at up to 35 kWe/wt%$_H$. This is sensible, as the molecular weight of hydrogen results in a relatively large molar contribution per incremental unit of mass compared to carbon

or oxygen. Fuel hydrogen near 6 wt % represents an unstable operating condition in the direction of decreasing hydrogen.

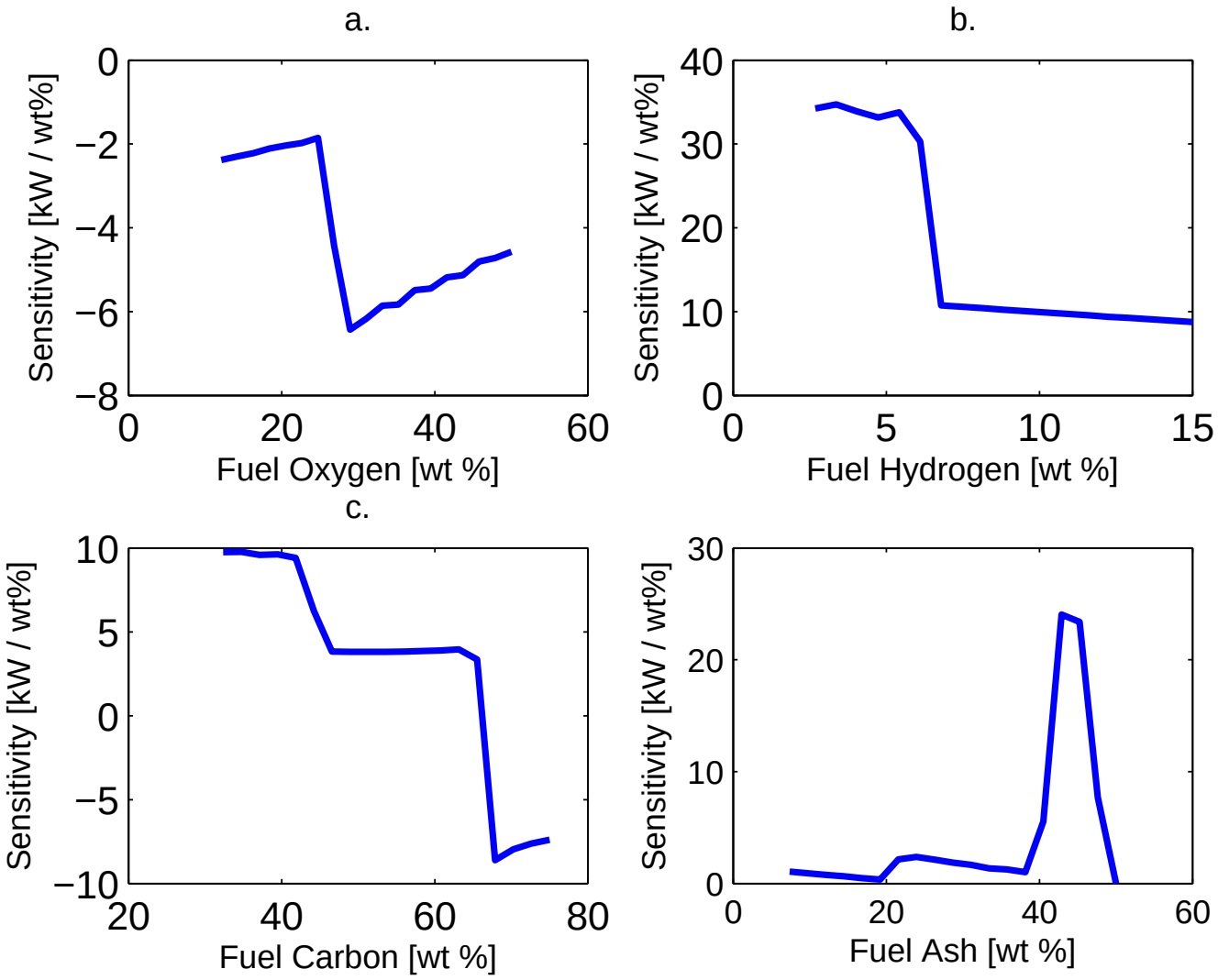

Figure 3.12: Sensitivity of net power to fuel composition. Plots show the numerical partial derivative of net power output for the selected species. Fuel composition was varied by adjusting the mass percentage of the selected species while holding the relative amount of all other species constant. Plot a: O_2, b: H_2, c: carbon, d: ash (non-reactive).

Fuel carbon is a reduced species and represents available chemical energy. Net power output is seen to increase with fuel carbon up to 68 wt %. The effect is shown in Figure 3.11c. The large stable operating range with a 3 kW/$\%_C$ slope fortunately captures the carbon content of most sludges. Above 68 wt % carbon, insufficient oxygen exists for complete

gasification. The air admitted for partial combustion is controlled only by gasification temperature. The negative sensitivity beginning at 68 wt % carbon is manifested as decreasing η_c. This model is therefore not capable of simulating coal in its current form. However, the general trend that increased carbon serves to increase net power stands for biomass fuels where the mass fraction of carbon is generally under 60 wt %.

Fuel ash has no effect on gasification chemistry in this simplified model. In actual systems biomass ash, including wastewater sludge ash, can catalyze the cracking of tar species into lighter molecules. Operationally, this suggests that less chemical energy in the form of tars will be lost to the wet scrubber. Otherwise, ash only serves as a heat sink which is heated in the gasifier then disposed of without energy recovery. Ash content also takes the place of organic molecules which would contribute to the mass basis LHV of sludge. It should be expected that increased ash has a negative impact on net power output. Simulation results, Figure 3.11, bear this out. Net power slowly decreases to about 40 wt % where net power output falls quickly to zero. At this point there is insufficient chemical energy in the sludge as $\dot{m}_{\text{sludge}} LHV_{\text{sludge}}$ to satisfy system heat loads. Most biomass sources including wood and agricultural waste have ash contents below 10 wt %. Sludge is unique amongst fuels with ash contents between 25 wt % and 45+ wt %. High ash sludges may not be amenable to thermochemical conversion approaches to energy recovery.

The sensitivity results show that energy recovery is greatest with low oxygen, high hydrogen fuels with a low ash content. TCC approaches may not be applicable for high ash, high oxygen fuels. Knowledge of the system sensitivity throughout the range of fuel composition can also inform the system design basis. Where average fuel properties are near steep-slope regions in net power output, system design can be based on the most conservative fuel composition. Extrapolating past the system boundary, the sensitivity analysis can inform WWTP process design. It may be possible to approach energy net-zero WWTP operation by careful upstream process design. Designing processes to use minimum aeration and pumping energy reduces WWTP energy demand. Novel wastewater treatment processes

such as enhanced primary clarification [23] may allow more sewage organic material to be recovered in sludge rather than consumed by microbial metabolism. Such approaches create sludges higher in carbon and hydrogen content, thereby increasing the potential electrical power recovered.

3.7 Effect of Carbon Conversion Efficiency

Optimization studies (Section 3.2) show that the system may be sensitive to carbon conversion efficiency, η_C. Some sensitivity is expected as unconverted carbon reflects chemical energy that is left out of the syngas stream. An additional motivation for exploring this sensitivity is that η_C has been assumed to be temperature dependent only, while in a real system it is dependent upon many factors. The effect of varying η_C from 50 % to 95 % is shown in Figure 3.13. The trend is generally linear with a sensitivity, or slope, or 2.72 kW/%. This result is fortunate. η_C is difficult to estimate and some laboratories have measured low η_C for air gasification of wastewater sludge [96]. Comparing this result with Figure 3.15 suggests that economic feasibility will be maintained even if η_C in a real system is substantially lower than the values used by the simulation. Overall, it seems that the system is not sufficiently sensitive to η_C to jeopardize the economic feasibility conclusions given in Section 3.10.

3.8 Effect of Raw Sludge Moisture

A final sensitivity study was done to investigate the effect of initial moisture on net power output. Sludge is commonly produced at about 95 wt % water on a wet basis [4]. Most thermochemical processes which are capable of producing net energy demand fuel moisture less than about 30 wt %. In fact, as reported in Table 3.6, despite a highly diluted syngas the 10 wt% moisture fueled air process outperforms the steam process with 28 wt % fuel moisture. At low moisture concentrations this analysis has shown that drying energy can have a dominant effect on system performance (see Figure 2.1). Figure 3.14 shows the effect of varying raw sludge moisture supplied to the dryer.

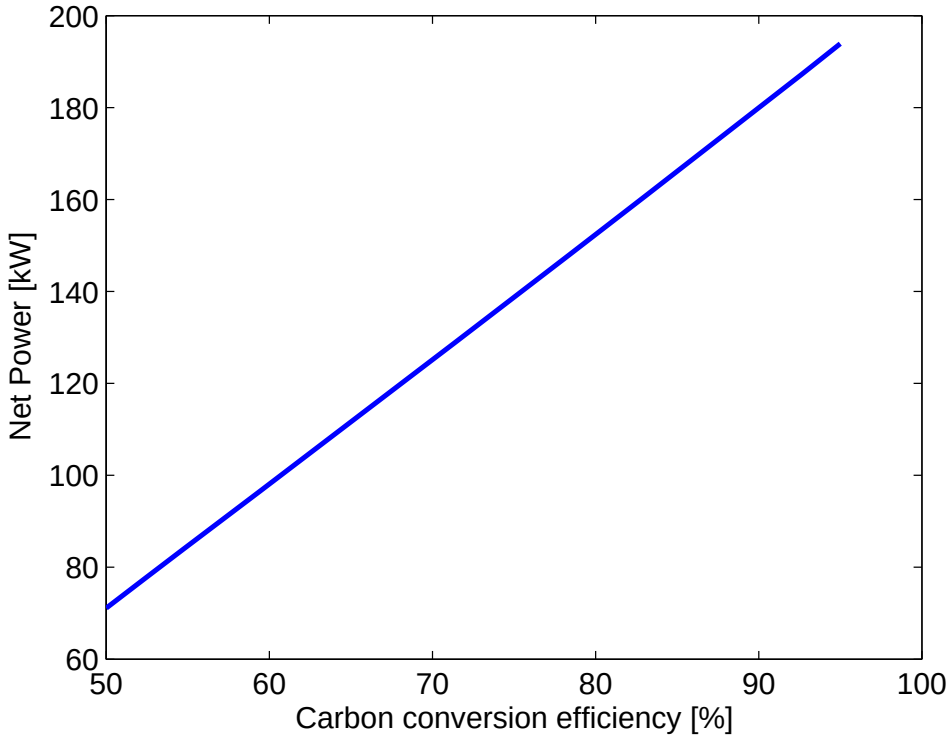

Figure 3.13: Effect of carbon conversion efficiency, η_c, on air process net power output. η_c varied between 50 % and 95 % holding all other parameters constant. T_{gasif} = 850 °C, post-dryer moisture = 10 wt %, $\dot{m}_{sludge}$ = 5 dry ton/day.

As expected, net power output is maximized for the lowest raw sludge moisture content. In in the linear region from 80 wt % to 10 wt % (for clarity the plot does not show moisture content less than 70 wt %) the net power changes only by about 100 $W/\%_{H_2O}$ with a maximum output of about 180 kW at 10 wt % moisture. However, at very low moisture levels the system tolerates lower gasifier operating temperatures as drying energy can be satisfied entirely by engine exhaust heat. Reduced gasifier operating temperature allows for a lower air process ER and lower indirect heating requirements by the steam process. Moisture levels above about 80 wt % quickly drive net power output to zero for drying by thermal means only. Generally, it is impossible to operate the model system for raw sludge moisture above 85 wt % without using more energy efficient mechanical drying to bring initial moisture to 80 wt % or less. This approach was used in the project scope, where a centrifuge reduces raw sludge moisture content to 80 wt % before crossing the system boundary.

Unfortunately, in most cases it is not possible to achieve less than 80 wt % moisture without thermal drying. Mechanical drying technologies except for filter presses cannot achieve moisture levels below 80 wt % [4]. Filter presses are available which can reduce moisture below 60 wt % and may be an option to system design. Such presses are typically batch operations and require operator and maintenance attention to a greater degree than a centrifuge. Other methods of sludge pre-drying such as open solar or greenhouse solar drying are probably not applicable to urban WWTPs where the odor and footprint of such methods would be prohibitive.

3.9 Technical Feasibility

This analysis has determined that electrical generation based on the air gasification of wastewater sludge is indeed feasible. In order to support the thermodynamic conclusions a technical analysis was conducted to determine if the system design is technically feasible to construct and operate. Sewage sludge properties are variable, with organic and inorganic compositions that depend upon numerous factors including WWTP process design, geography, time of day and year, upstream plant conditions, etc. An additional complication comes

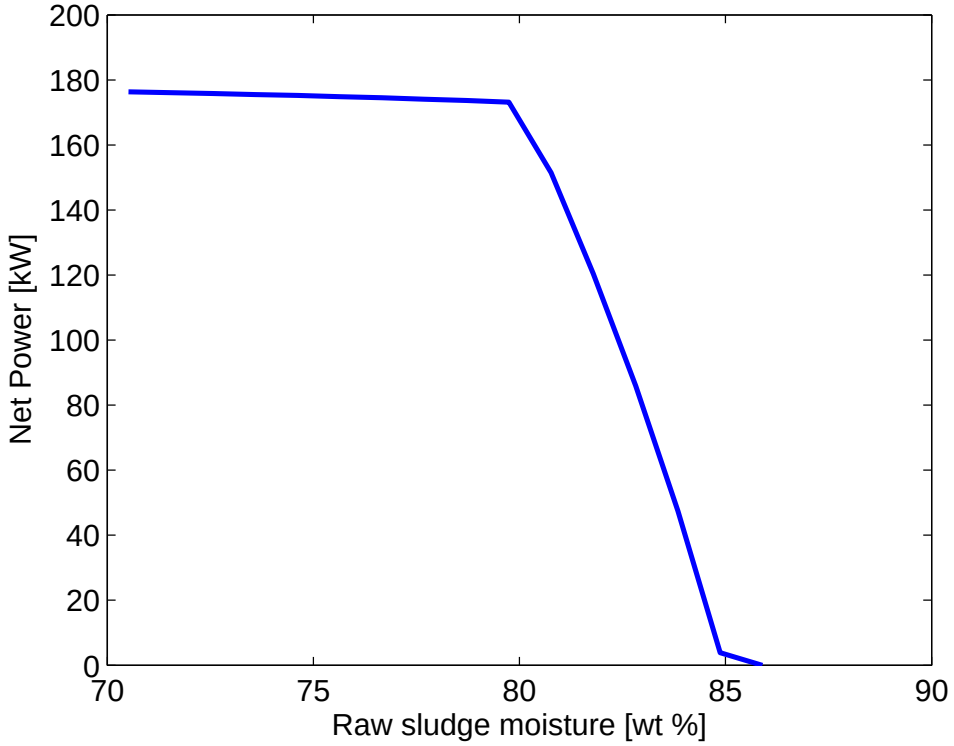

Figure 3.14: Effect of raw sludge moisture content on air process net power output. Raw sludge moisture taken as moisture content of sludge fed to the dryer, not necessarily as produced by the WWTP. Moisture varied between 70 wt % and 86 wt % holding all other parameters constant. Moisture content above 86 wt % is energetically infeasible and not shown. Moisture content less than 70 wt % continues the linear portion of the curve with a maximum output of 180 kW at 10 wt %. T_{gasif} = 850 °C, post-dryer moisture = 10 wt %, $\dot{m}_{sludge}$ = .058 dry kg/s.

from limited commercial experience with thermochemical conversion of sludge, especially at a small scale. Where sludge specific components were not available, the analysis used data from general biomass sources with the assumption that this technology is likely adaptable to sludge service.

Feedstock drying and conveyance may pose the greatest mechanical challenges to system design. Sludge enters the system boundary at 80 wt % water in pumpable slurry. The air-and steam-blown gasification processes described above require fuel moisture of 10 wt % and 28 wt % respectively. Mechanical dewatering approaches such as centrifuges and belt presses are generally incapable of reducing moisture below 75 wt % [4]. Some filter presses are available which can reduce moisture below 75 wt % but they are nonetheless unable to achieve the moisture concentrations needed for the system specifications. Thus, even where mechanical dewatering is incorporated as a first step, full drying must be accomplished by thermal means.

Two general classes of thermal dryers are available which can readily dry sludge to <10 wt % water. Direct, or convective, dryers contact sludge with hot drying gas. Evaporated water is entrained in the drying gas. Sludge transport is often by belts or flights in a rotating drum. Fluidized bed direct dryers are also available but are not cost effective at small scale [24]. Direct dryers can operate at relatively low temperatures, even below 200 °C [101], by accepting large mass flows of drying gas. This is useful where low temperature waste heat sources are available. Downsides to direct drying include potentially large volume and concomitant surface heat losses along with high cost. Indirect dryers operate in the 300 °C-400 °C or greater temperature range by circulating a heat transfer fluid through a jacketed chamber. Conduction from the chamber wall raises the temperature of sludge above 100 °C, evaporating water. Such dryers tend to transport sludge with scrapers or screw feed mechanisms. Downsides to indirect drying are the need for a relatively high temperature heat source and risk of explosion due to high temperatures causing volatile organic molecules to entrain in the dryer exhaust. Regardless of the drying technology a saturated, malodorous

exhaust gas stream exits the dryer. Dryer gas scrubbing will likely be necessary. Water scrubbers offer a highly effective, simple solution to condense water and organics from the dryer exhaust stream before stack discharge. It is anticipated that the water demanded by the dryer exhaust scrubber would not pose a problem to a WWTP.

Sludges of moisture concentration below 15 wt % can be considered granular material and are easily handled. However, sludges between 15 wt % and 60 wt% water exhibit a non-Newtonian sticky consistency [72]. Discussion with sludge conveyance equipment vendors including Andritz, Komline-Sanderson, and RUF suggest that sludges of 28 wt % moisture may not be conveyable. Re-designing the steam process to dry sludge to 15 % and supply the necessary steam from a utility boiler reduces process efficiency and net electrical output further below that of the air process.

The final components involved in sludge handling are the briquetter (for fixed bed gasifiers) and fuel charging equipment. The dry, granular solids required by the air process are readily briquetted by available equipment. Depending on sludge characteristics and briquette strength requirements a binder may be required. Gasifier charging equipment design depends upon the type of reactor. Downdraft, co-flowing air blown gasifiers may be gravity fed by simple metering hoppers or conveyors. Charging downdraft gasifiers should be simple and robust for briquettes of dry fuel. Fluidized bed gasifiers operate on small particulate fuel, usually no briquetting is necessary. However fluidized beds require more sophisticated charging apparatus [24]. Even at net atmospheric pressure, high velocity fluidization gas creates a pressure difference across the reactor which requires any charging system to be gas-tight. Further, the charging apparatus is likely to be near the bed or in the freeboard of the reactor, both of which are at high temperature. Fuel must be admitted to the gasifier in such a way that it does not begin to pyrolyze before entering the gasifier. Common approaches are lock hoppers with screw feeders, piston pumps, and rotary valves [24]. Each of these methods generally requires cooling water and some combination of compressed air, steam, or nitrogen to rapidly discharge fuel. The technical challenges and mechanical complexity

of charging fuel to fluidized bed reactors suggests these systems will be more expensive and require more operator attention than the simpler briquette charging apparatus needed by fixed bed reactors.

Numerous gasifier designs have been developed [51]. This analysis considers only the fixed bed downdraft gasifier and the bubbling fluidized bed gasifier. Both reactors are applicable to small scale systems and represent the overall best cost effectiveness system-wide. The fixed bed downdraft gasifier supports a continuously replenished fuel pile on top of an ash grate. Fresh fuel is charged from the top of the reactor and proceeds through drying, pyrolysis, and combustion zones as it travels downward toward the ash grate. Combustion air is drawn through the bed and usually also injected via controlled tuyéres in the combustion zone. Syngas contact with char on the ash grate acts to filter many contaminants, producing a low tar syngas with limited heavy metal entrainment. Hot ash additionally serves to catalyze tar cracking reactions [47]. Syngas is drawn from the bottom of the reactor, which also holds ash withdrawal machinery. Fixed bed reactors are limited in scale, as reactor dimensions increase the chance of developing gas channels and/or hot spots also increases. Both phenomena greatly reduce gasification efficiency. In a bubbling fluidized bed reactor a mixture of fuel and fine sand or refractory catalyst is fluidized by forcing gasification medium across the bed. The resulting high mixing efficiency ensures efficient heat and mass transfer. Syngas is drawn from the top of the reactor with some entrained char and bed material. A cyclone separates solids and discharges syngas. Fluidized bed reactor systems are more complex than fixed beds with greater parasitic energy demand from the fluidization blower. Additionally control systems must be in place to maintain bed levels, and bed material will need occasional replacement as it is ejected with waste char.

From the perspective of small-scale generation the mechanically simple fixed bed downdraft reactor is the superior choice. This reactor can be charged with reliable and simple briquette feeding machinery and eliminates the need for a fluidization blower and char cyclone. Biomass gasification in downdraft reactors is established in practice [51]. Henriksen

and colleagues [102] operated a small scale, high temperature wood-fired downdraft research gasifier. They found no significant corrosion or operational issues. It must be stressed however that the inorganic content of sludge is quite different from common biomass. Further research should be undertaken to determine the effects of sewage sludge ash at high temperature on reactor metallurgy. Ash fusion is unlikely to pose a problem for operating temperatures around 850 °C. Kupka [97] measured ash fusion in a gasifier for different coal and biomass sources. Sludge ash was not found to soften until 1100 °C.

Processes downstream of the gasifier are not expected to be unusually challenged by sludge fuel in comparison to common biomass fuels. However such equipment may necessarily be specialized and costly. For example, the syngas heat exchanger and associated piping must be constructed of corrosion resistant materials to accommodate high temperature hydrogen and the possibility of water condensation during start-up and shutdown. Also, special consideration must be given to the internal combustion engine to ensure its compatibility with low LHV syngas. Nevertheless, equipment for all processes downstream of the gasifier is found to be commercially available from process equipment suppliers. Overall, technical considerations suggest that the air gasification process with 10 wt % dried solids is technically feasible.

3.10 Economic Feasibility

This analysis shows it is technically and energetically possible to produce net electrical power from the air blown gasification of wastewater sludge. Whether this technology can be successfully applied in decentralized wastewater treatment plants depends upon economic considerations. On-site electricity generation allows for value recovery by reducing utility purchases. Further savings can be realized by relieving the costs associated with sludge stabilization and disposal. In order for a gasification plant to be economically viable the savings from generated electricity and reduced disposal cost must offset the capital investment and manufacturing costs incurred by the plant. WWTP capacities are investigated in the range of 0.5 to 5 dry metric tons of sludge per day. This corresponds to a WWTP capacity of

0.55-5.5 million gallons per day (MGD) [1]. A benchmarking analysis compares the major equipment costing method to a commercially available wood-fired, small-scale gasifier platform manufactured by a Colorado-based biomass energy company (Community Power Corporation 2012).

Table 3.9: Results of economic analysis

WWTP Capacity MGD	**Present Worth $ Thousand**	**TCI $ Thousand**
0.55	-1604	165
1.1	-767	254
2.2	1053	387
2.2	Incl. Dryer	1,100
3.3	3154	505
4.4	5110	598
5.5	7106	674

Table 3.9 shows the results of the economic evaluation. PW of the gasification plant, in comparison to the base case, becomes economically viable at a plant capacity of about 2.2 MGD (0.115 m3/s). Over a plant lifetime of 20 years, the 2.2 MGD plant will earn about $1,053,000 over the base case. Profit margins at this level allow for some confidence in covering unanticipated costs. To benchmark this cost analysis, the TCI of the modeled gasifier plant is compared to a highly automated, turnkey biomass gasification platform produced by Community Power Corporation (CPC). The CPC system delivers 100 kWe from wood fuel at a cost of $1.2 million commissioned. Small-scale gasifier plants are available from companies including Gasek and All Power Labs however the sophisticated CPC system is a closer match to this system design. The modeled sludge gasification system (including dryer cost) at capacity equivalent to the CPC system is expected to cost $ 1.1 million. The present worth calculation in Table 3.9 shows gasification plant cost, or TCI, compared to the base case where the cost of drying machinery is cancelled (see Section 2.8). Close agreement

between modeled costs and the commercial system supports the validity of the costing model. Further engineering effort will likely decrease system cost and increase the range of economic feasibility for decentralized WWTPs.

Since net electrical output, and thus economic viability, depend on numerous factors including fuel composition (section 3.6), PW of the 5.5 MGD system was analyzed for net power output between 100 and 200 kW for a 5 dry ton/day system (or about 5.5 MGD raw sewage flow). The system remains economically net positive even at 100 kWe net output, or about 30 % less than the design basis. Over the 20 year plant service life a 100 kWe gasification plant in a 5.5 MGD WWTP should produce nearly $5.7 million. Present worth as a function of net power is presented in Figure 3.15. The trend holds for other plant capacities. Generally, economic viability holds for net power decreased to 30 % below the simulated performance.

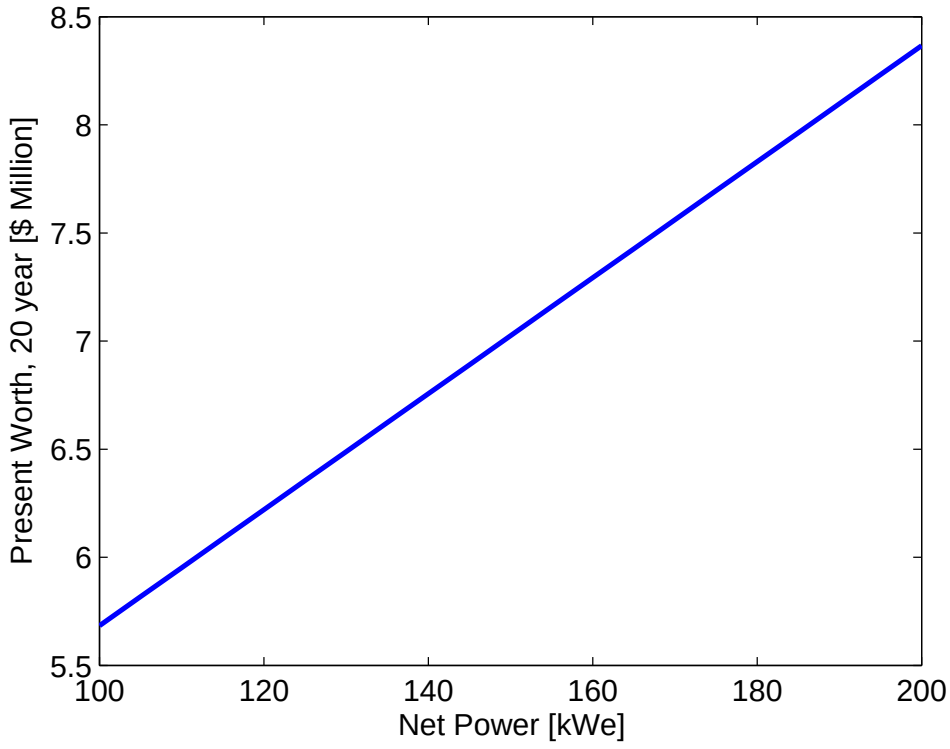

Figure 3.15: Present worth as a function of electrical output

Recall from Section 2.8 that the cost factor method is generally accurate to ± 30 %. For the 2.2 MGD plant, PW at +30 of model cost % is $670,000 and PW for -30 of model cost % cost is $1,435,000. Thus, the economic feasibility conclusions are stable against costing method uncertainty. Overall, the fuel cost incurred by the base case drives economic viability. The conclusion that economic viability is driven by consumption of a commodity (natural gas) creates a potential confound. Commodity prices are likely to be less stable than capital machinery cost. More advanced economic viability analyses for a potential capital project must account for natural gas price trends. The 2.2 MGD plant is no longer economically viable if natural gas cost is reduced by 33 %. However, in this case natural gas cost in the U.S. is depressed by supply from enhanced recovery technologies. As more industries and utilities switch to natural gas firing and export facilities come online, natural gas cost will likely increase, further supporting economic viability.

Considering the effect natural gas cost can have on economic feasibility, an additional design option is co-fueling with natural gas. Natural gas may be used as an amendment to syngas or as a heat source for drying or gasifier heating. Results (Section 3.2) show that the air process syngas LHV is about 4 MJ/kg. Literature review suggests that stable combustion of syngas may be difficult at such a low LHV. Engine efficiency will also be less than the name plate value. Blending natural gas with the air process syngas was proven to increase efficiency and combustion stability [83]. Use of natural gas to heat the gasifier or dryer would result in all syngas being consumed by the engine-generator. Co-fueling may allow the system to remain economically viable if low natural gas or utility electricity costs render the system economically infeasible as a stand-alone generating system.

Overall, this analysis has demonstrated that the simulated system is economically viable for WWTPs with raw sewage flows of about 2.2 MGD. The conclusion holds for initial cost estimates of ± 30 % and net power output 30 % below the simulated value.

3.11 Opportunities for Future Work

This particular research effort was only intended to explore the feasibility of a gasification-based electrical generation process at small, urban WWTPs from a high level, general perspective. However, the long-term goal of this line of research is to facilitate the implementation of a sludge-to-energy process at real WWTPs. The positive feasibility analyses reported herein suggests that practical implementation of the technology may indeed be possible. As a feasibility analysis is only the first step in developing a new process, opportunities for further work remain.

Many of the outstanding questions pertain to gasifier operation. First, the effect of inorganic species must be studied. In the interest of environmental responsibility and permit requirements, the fate of heavy metals is of great concern. In particular, whether metals entrain in the syngas, bind to char and ash, or present a corrosion risk. Furthermore, it must be determined whether metals are can be leached from ash. If ash does not adequately sequester heavy metals, gasification ash may be considered a hazardous material and require specialized disposal. Experimental studies must also be conducted to determine the role of alkali metals and salts in corrosion and fouling of gas-contact surfaces. The final unknowns regarding inorganic content that are recognized at this point are ash slagging and catalytic activity. Ash softening and agglomerating on fuel particles could greatly reduce gasification efficiency. However, ash in solid form may be able to catalytically crack tar precursors and produce a relatively clean syngas.

The remaining questions at this point center around system simulation. The system models were developed to neglect the performance characteristics of real components. Furthermore, gasifier chemistry was approximated using equilibrium calculations. Completely general chemical kinetic models are probably impossible to develop, however global kinetics for a specific reactor type may be possible to approximate. A global kinetics model would be able to provide more accurate syngas chemistry data. In addition to enhanced syngas composition data, simulations incorporating the performance characteristics of real compo-

nents are needed to generate more accurate net power output calculations. Essentially, from a modeling perspective, the analysis would benefit by representing a real system using chemistry data from a downdraft-type experimental reactor rather than a simple thermodynamic approximation.

A well developed system model incorporating empirical chemistry data and the performance characteristics of real components would provide high-confidence estimates of net power output and economic feasibility. However, wastewater sludges have a widely variable composition. The effect of different sludge characteristics must be studied experimentally in order to determine overall feasibility for a given WWTP. In particular, the characteristics which cannot be approximated in the model, such as the ability of dried sludge to pelletize, actual carbon conversion efficiency, the effect of variable inorganic composition, etc., should be investigated experimentally using standardized procedures.

CHAPTER 4

CONCLUSION

Overall, this analysis has shown that a decentralized urban wastewater treatment plant can cost-effectively apply air blown gasification technology to produce on-site electrical power and stabilize a hazardous waste stream. Wastewater treatment plants with raw sewage flows of 2.2 MGD or greater can realize a 20 year profit of about $1,000,000 with a net electrical power output of about 60 kW. Moreover, the technology proves to be economically viable at small scale. The conclusions reached herein have added to the knowledge base of small biomass cogeneration system design and simulation. In particular, small scale sewage sludge cogeneration has been investigated on a systems level; a topic which has no literature support as of this writing. This systems-level analysis has proven the applicability of restricted equilibrium gasifier chemistry models to predicting power output of a cogeneration system, provided experimental work to calibrate the model exists. This is an important result for analysis of biomass waste. Essentially, the feasibility of gasification-cogeneration on any fuel which can be described by a proximate and ultimate analysis can be estimated without detailed knowledge of chemical processes occurring in reactor. However it must be stressed that simple thermochemical analyses have no predictive power over actual reactor operating conditions, such as the effects of corrosive gasification products or ash management challenges. The fact that this analysis concludes that wastewater sludge cogeneration at small scale is economically feasible even with $\pm$ 30 % costing accuracy should motivate academic and industrial development. Application of this technology promises to reduce operating costs of wastewater treatment plants, carbon emissions from fossil-fired electricity, and the quantity of sludge requiring land disposal.

REFERENCES CITED

[1] L Metcalf, H. P. Eddy, and G Tchobanoglous. *Wastewater engineering: treatment, disposal, and reuse.* McGraw Hill, 2010.

[2] Biosolids Generation. Use, and disposal in the united states. 1999.

[3] Ashley Murray, Arpad Horvath, and Kara L. Nelson. Hybrid life-cycle environmental and cost inventory of sewage sludge treatment and end-use scenarios: a case study from china. 42(9):31633169, 2008. URL http://pubs.acs.org/doi/abs/10.1021/es702256w.

[4] J. Werther and T. Ogada. Sewage sludge combustion. 25(1):55116, 1999. URL http://www.sciencedirect.com/science/article/pii/S0360128598000203.

[5] S. Werle and R. K. Wilk. A review of methods for the thermal utilization of sewage sludge: The polish perspective. 35(9):19141919, 2010. URL http://www.sciencedirect.com/science/article/pii/S0960148110000364.

[6] D. Fytili and A. Zabaniotou. Utilization of sewage sludge in EU application of old and new methodsA review. 12(1):116–140, January 2008. ISSN 13640321. doi: 10.1016/j.rser.2006.05.014. URL http://linkinghub.elsevier.com/retrieve/pii/S1364032106000827.

[7] W. Rulkens. Sewage sludge as a biomass resource for the production of energy: Overview and assessment of the various options. 22(1):915, 2007. URL http://pubs.acs.org/doi/abs/10.1021/ef700267m.

[8] A. V. Bridgwater. The technical and economic feasibility of biomass gasification for power generation. 74(5):631653, 1995. URL http://www.sciencedirect.com/science/article/pii/001623619500001L.

[9] G. Houillon and O. Jolliet. Life cycle assessment of processes for the treatment of wastewater urban sludge: energy and global warming analysis. 13(3):287299, 2005. URL http://www.sciencedirect.com/science/article/pii/S0959652604000976.

[10] D. T. Furness, L. A. Hoggett, and S. J. Judd. Thermochemical treatment of sewage sludge. 14(1):5765, 2000. URL http://onlinelibrary.wiley.com/doi/10.1111/j.1747-6593.2000.tb00227.x/abstract.

[11] P. Manara and A. Zabaniotou. Towards sewage sludge based biofuels via thermochemical conversion a review. 16(5):2566–2582, June 2012. ISSN 13640321. doi: 10.1016/j.rser.2012.01.074. URL http://linkinghub.elsevier.com/retrieve/pii/S136403211200086X.

[12] E.E. Kwon, H. Yi, and H.H. Kwon. Urban energy mining from sewage sludge. 90(4): 1508–1513, January 2013. ISSN 00456535. doi: 10.1016/j.chemosphere.2012.07.062. URL http://linkinghub.elsevier.com/retrieve/pii/S0045653512010053.

[13] M. Verma, S. Godbout, S. K. Brar, O. Solomatnikova, S. P. Lemay, and J. P. Larouche. Biofuels production from biomass by thermochemical conversion technologies. 2012: 1–18, 2012. ISSN 1687-806X, 1687-8078. doi: 10.1155/2012/542426. URL http://www.hindawi.com/journals/ijce/2012/542426/.

[14] S. D. Probert, K. Kerr, and J. Brown. Harnessing energy from domestic, municipal and industrial refuse. 27(2):89168, 1987. URL http://www.sciencedirect.com/science/article/pii/0306261987900171.

[15] A. V. Bridgwater. Renewable fuels and chemicals by thermal processing of biomass. 91(2):87102, 2003. URL http://www.sciencedirect.com/science/article/pii/S1385894702001420.

[16] Ryan M. Swanson, Justinus A. Satrio, Robert C. Brown, Alexandru Platon, and David D. Hsu. Techno-economic analysis of biofuels production based on gasification. 303:2753000, 2010. URL http://www.nrel.gov/docs/fy11osti/46587.pdf.

[17] Robert J. Braun, Luke G. Hanzon, and Jered H. Dean. System analysis of thermochemical-based biorefineries for coproduction of hydrogen and electricity. 133(1):012601, 2011. ISSN 01950738. doi: 10.1115/1.4003541. URL http://EnergyResources.asmedigitalcollection.asme.org/article.aspx?articleid=1415099.

[18] Anastasia M. Gribik, Ronald E. Mizia, Harry Gatley, and Benjamin Phillips. Economic and technical assessment of wood biomass fuel gasification for industrial gas production. Technical report, Technical report of Idaho National Laboratory INL/EXT-07-13292, 2007. URL http://www.inl.gov/technicalpublications/Documents/3787330.pdf.

[19] Margaret K Mann and Pamela L Spath. Life cycle assessment of a biomass gasification combined cycle system.pdf. Technical Report NREL/DE-AC36-83CH10093, National Renewable Energy Lab., Golden, CO (United States), 2007.

[20] K Choy, J Porter, C Hui, and G Mckay. Process design and feasibility study for small scale MSW gasification. 105(1-2):31–41, December 2004. ISSN 13858947. doi: 10.1016/j.cej.2004.07.012. URL http://linkinghub.elsevier.com/retrieve/pii/S1385894704003018.

[21] U. Arena, F. Di Gregorio, and M. Santonastasi. A techno-economic comparison between two design configurations for a small scale, biomass-to-energy gasification based system. 162(2):580–590, August 2010. ISSN 13858947. doi: 10.1016/j.cej.2010.05.067. URL http://linkinghub.elsevier.com/retrieve/pii/S138589471000522X.

[22] Weerachai Arjharn, Thipsuphin Hinsui, Pansa Liplap, and G. S. Vijaya Raghavan. Evaluation of an energy production system from sewage sludge using a pilot-scale downdraft gasifier. 27(1):229–236, January 2013. ISSN 0887-0624, 1520-5029. doi: 10.1021/ef3012728. URL http://pubs.acs.org/doi/abs/10.1021/ef3012728.

[23] Dotti F. Ramey, Nicholas P.G. Lumley, Greta Buschmann, Ana Lucia Prieto, Jason M. Porter, and Tzahi Y. Cath. Evaluation of the suitability of wastewater solids for gasification in urban decentralized water reclamation facilities.

[24] Keith R. Cummer and Robert C. Brown. Ancillary equipment for biomass gasification. 23(2):113128, 2002. URL http://www.sciencedirect.com/science/article/pii/S0961953402000387.

[25] A.V. Bridgwater. Review of fast pyrolysis of biomass and product upgrading. 38: 68–94, March 2012. ISSN 09619534. doi: 10.1016/j.biombioe.2011.01.048. URL http://linkinghub.elsevier.com/retrieve/pii/S0961953411000638.

[26] Isabel Fonts, Gloria Gea, Manuel Azuara, Javier brego, and Jess Arauzo. Sewage sludge pyrolysis for liquid production: A review. 16(5):2781–2805, June 2012. ISSN 13640321. doi: 10.1016/j.rser.2012.02.070. URL http://linkinghub.elsevier.com/retrieve/pii/S1364032112001657.

[27] M. Inguanzo, A. Domnguez, J. A. Menndez, C. G. Blanco, and J. J. Pis. On the pyrolysis of sewage sludge: the influence of pyrolysis conditions on solid, liquid and gas fractions. 63(1):209222, 2002. URL http://www.sciencedirect.com/science/article/pii/S0165237001001553.

[28] C. Franco, F. Pinto, I. Gulyurtlu, and I. Cabrita. The study of reactions influencing the biomass steam gasification process. 82(7):835842, 2003. URL http://www.sciencedirect.com/science/article/pii/S0016236102003137.

[29] C. Gai and Y. Dong. Experimental study on non-woody biomass gasification in a downdraft gasifier. 2012. URL http://www.sciencedirect.com/science/article/pii/S0360319911026838.

[30] M He, Z Hu, B Xiao, J Li, X Guo, S Luo, F Yang, Y Feng, G Yang, and S Liu. Hydrogen-rich gas from catalytic steam gasification of municipal solid waste (MSW): influence of catalyst and temperature on yield and product composition. 34(1):195–203, January 2009. ISSN 03603199. doi: 10.1016/j.ijhydene.2008.09.070. URL http://linkinghub.elsevier.com/retrieve/pii/S0360319908012342.

[31] National Research Council (US). Committee on Toxicants and Pathogens in Biosolids Applied to Land. *Biosolids applied to land: Advancing standards and practices*. Natl Academy Pr, 2002.

[32] A national biosolids regulation, quality, end use & disposal survey. Technical report, North East Biosolids and Residuals Association (NEBRA), 2007.

[33] Standards for the use or disposal of sewage sludge, August 1998.

[34] Peter McKendry. Energy production from biomass (part 2): conversion technologies. 83(1):4754, 2002. URL http://www.sciencedirect.com/science/article/pii/S0960852401001195.

[35] E. Cartmell, P. Gostelow, D. Riddell-Black, N. Simms, J. Oakey, J. Morris, P. Jeffrey, P. Howsam, and S. J. Pollard. Biosolids a fuel or a waste? an integrated appraisal of five co-combustion scenarios with policy analysis. 40(3):649658, 2006. URL http://pubs.acs.org/doi/abs/10.1021/es052181g.

[36] T. Lendormi, C. Prevot, F. Doppenberg, J.N. Foussard, and H. Debellefontaine. Subcritical wet oxidation of municipal sewage sludge: comparison of batch and continuous experiments. 44(5):161–169, 2001.

[37] Y Khan, G.K Anderson, and D.J Elliott. Wet oxidation of activated sludge. 33(7):1681–1687, May 1999. ISSN 00431354. doi: 10.1016/S0043-1354(98)00387-X. URL https://secure.mines.edu/science/article/pii/,DanaInfo=www.sciencedirect.com+S004313549800387X.

[38] J. W. Griffith and D. H. Raymond. The first commercial supercritical water oxidation sludge processing plant. 22(4):453459, 2002. URL http://www.sciencedirect.com/science/article/pii/S0956053X02000296.

[39] J. Van Caneghem, A. Brems, P. Lievens, C. Block, P. Billen, I. Vermeulen, R. Dewil, J. Baeyens, and C. Vandecasteele. Fluidized bed waste incinerators: Design, operational and environmental issues. 2012. URL http://www.sciencedirect.com/science/article/pii/S0360128512000160.

[40] David Brown, Martin Gassner, Tetsuo Fuchino, and Franois Marchal. Thermo-economic analysis for the optimal conceptual design of biomass gasification energy conversion systems. 29(11-12):2137–2152, August 2009. ISSN 13594311. doi: 10.1016/j.applthermaleng.2007.06.021. URL http://linkinghub.elsevier.com/retrieve/pii/S1359431107002232.

[41] D. Vamvuka. Bio-oil, solid and gaseous biofuels from biomass pyrolysis processes-an overview. 35(10):835–862, August 2011. ISSN 0363907X. doi: 10.1002/er.1804. URL http://doi.wiley.com/10.1002/er.1804.

[42] Mark M. Wright, Justinus A. Satrio, Robert C. Brown, Daren E. Daugaard, and David D. Hsu. Techno- economic analysis of biomass fast pyrolysis to transportation fuels. Technical Report NREL/TP-6A20-46586, National Renewable Energy Lab., Golden, CO (United States), 2010.

[43] Y. Kim and W. Parker. A technical and economic evaluation of the pyrolysis of sewage sludge for the production of bio-oil. 99(5):14091416, 2008. URL http://www.sciencedirect.com/science/article/pii/S096085240700154X.

[44] Nimit Nipattummakul, Islam Ahmed, Somrat Kerdsuwan, and Ashwani K. Gupta. High temperature steam gasification of wastewater sludge. 87(12):3729–3734, December 2010. ISSN 03062619. doi: 10.1016/j.apenergy.2010.07.001. URL http://linkinghub.elsevier.com/retrieve/pii/S0306261910002540.

[45] Y. Yang, J.G. Brammer, M. Ouadi, J. Samanya, A. Hornung, H.M. Xu, and Y. Li. Characterisation of waste derived intermediate pyrolysis oils for use as diesel engine fuels. 103:247–257, January 2013. ISSN 00162361. doi: 10.1016/j.fuel.2012.07.014. URL http://linkinghub.elsevier.com/retrieve/pii/S0016236112005637.

[46] Eoin Butler, Ger Devlin, Dietrich Meier, and Kevin McDonnell. A review of recent laboratory research and commercial developments in fast pyrolysis and upgrading. 15 (8):4171–4186, October 2011. ISSN 13640321. doi: 10.1016/j.rser.2011.07.035. URL http://linkinghub.elsevier.com/retrieve/pii/S1364032111002759.

[47] L. Shen and D. K. Zhang. An experimental study of oil recovery from sewage sludge by low-temperature pyrolysis in a fluidised-bed< sup></sup>. 82(4):465472, 2003. URL http://www.sciencedirect.com/science/article/pii/S0016236102002946.

[48] Bert Van de Beld, Elmar Holle, and Jan Florijn. The use of pyrolysis oil and pyrolysis oil derived fuels in diesel engines for CHP applications. 102:190–197, February 2013. ISSN 03062619. doi: 10.1016/j.apenergy.2012.05.047. URL http://linkinghub.elsevier.com/retrieve/pii/S0306261912004205.

[49] David Chiaramonti, Anja Oasmaa, and Yrj Solantausta. Power generation using fast pyrolysis liquids from biomass. 11(6):1056–1086, August 2007. ISSN 13640321. doi: 10.1016/j.rser.2005.07.008. URL http://linkinghub.elsevier.com/retrieve/pii/S1364032105000997.

[50] M. Baratieri, P. Baggio, B. Bosio, M. Grigiante, and G.A. Longo. The use of biomass syngas in IC engines and CCGT plants: A comparative analysis. 29(16):3309–3318, November 2009. ISSN 13594311. doi: 10.1016/j.applthermaleng.2009.05.003. URL http://linkinghub.elsevier.com/retrieve/pii/S1359431109001446.

[51] Peter McKendry. Energy production from biomass (part 3): gasification technologies. 83(1):5563, 2002. URL http://www.sciencedirect.com/science/article/pii/S0960852401001201.

[52] Christopher Higman and van der Burgt. *Gasification*. Gulf, 2 edition, 2008.

[53] E. Biagini, F. Lippi, L. Petarca, and L. Tognotti. Devolatilization rate of biomasses and coalbiomass blends: an experimental investigation. 81(8):10411050, 2002. URL http://www.sciencedirect.com/science/article/pii/S0016236101002046.

[54] J. A. Conesa, A. Marcilla, R. Moral, J. Moreno-Caselles, and A. Perez-Espinosa. Evolution of gases in the primary pyrolysis of different sewage sludges. 313(1):6373, 1998. URL http://www.sciencedirect.com/science/article/pii/S0040603197004747.

[55] M.E. Snchez, J.A. Menndez, A. Domnguez, J.J. Pis, O. Martnez, L.F. Calvo, and P.L. Bernad. Effect of pyrolysis temperature on the composition of the oils obtained from sewage sludge. 33(6-7):933–940, June 2009. ISSN 09619534. doi: 10.1016/j.biombioe.2009.02.002. URL http://linkinghub.elsevier.com/retrieve/pii/S0961953409000385.

[56] Juan Manuel de Andres, Adolfo Narros, and Mara Encarnacin Rodrguez. Air-steam gasification of sewage sludge in a bubbling bed reactor: Effect of alumina as a primary catalyst. 92(3):433–440, March 2011. ISSN 03783820. doi: 10.1016/j.fuproc.2010.10.006. URL http://linkinghub.elsevier.com/retrieve/pii/S0378382010003541.

[57] Bodo Gro, Christian Eder, Peter Grziwa, Juri Horst, and Klaus Kimmerle. Energy recovery from sewage sludge by means of fluidised bed gasification. 28(10):1819–1826, January 2008. ISSN 0956053X. doi: 10.1016/j.wasman.2007.08.016. URL http://linkinghub.elsevier.com/retrieve/pii/S0956053X07002735.

[58] Thana Phuphuakrat, Nimit Nipattummakul, Tomoaki Namioka, Somrat Kerdsuwan, and Kunio Yoshikawa. Characterization of tar content in the syngas produced in a downdraft type fixed bed gasification system from dried sewage sludge. 89(9):2278–2284, September 2010. ISSN 00162361. doi: 10.1016/j.fuel.2010.01.015. URL http://linkinghub.elsevier.com/retrieve/pii/S0016236110000232.

[59] BioMax systems fact sheet, 2012.

[60] Jessica Francois, Lokmane Abdelouahed, Guillain Mauviel, Michel Feidt, Caroline Rogaume, Olivier Mirgaux, Fabrice Patisson, and Anthony Dufour. Estimation of the energy efficiency of a wood gasification CHP plant using aspen plus. 29:769774, 2012. URL http://www.academia.edu/download/30423287/129.pdf.

[61] Markus Bolhr-Nordenkampf, Reinhard Rauch, K. Bosch, C. Aichernig, and Hermann Hofbauer. Biomass CHP plant gssing-using gasification for power generation. page 567572, 2003. URL http://members.aon.at/biomasse/thailand.pdf.

[62] L. Fiori, M. Valbusa, and D. Castello. Supercritical water gasification of biomass for h2 production: Process design. 2012. URL http://www.sciencedirect.com/science/article/pii/S0960852412010322.

[63] Y. Calzavara, C. Joussot-Dubien, G. Boissonnet, and S. Sarrade. Evaluation of biomass gasification in supercritical water process for hydrogen production. 46(4):615631, 2005. URL http://www.sciencedirect.com/science/article/pii/S0196890404000949.

[64] Edgar Gasafi, Marion-Yvonne Reinecke, Andrea Kruse, and Liselotte Schebek. Economic analysis of sewage sludge gasification in supercritical water for hydrogen production. 32(12):1085–1096, December 2008. ISSN 09619534. doi: 10.1016/j.biombioe.2008.02.021. URL http://linkinghub.elsevier.com/retrieve/pii/S0961953408000482.

[65] Y Matsumura, T Minowa, B Potic, S Kersten, W Prins, W Vanswaaij, B Vandebeld, D Elliott, G Neuenschwander, and A Kruse. Biomass gasification in near- and super-critical water: Status and prospects. 29(4):269–292, October 2005. ISSN 09619534. doi: 10.1016/j.biombioe.2005.04.006. URL http://linkinghub.elsevier.com/retrieve/pii/S0961953405000735.

[66] G. P. Reed, N. P. Paterson, Y. Zhuo, D. R. Dugwell, and R. Kandiyoti. Trace element distribution in sewage sludge gasification: Source and temperature effects. 19(1):298–304, January 2005. ISSN 0887-0624, 1520-5029. doi: 10.1021/ef049943y. URL http://pubs.acs.org/doi/abs/10.1021/ef049943y.

[67] Th. Damartzis, S. Michailos, and A. Zabaniotou. Energetic assessment of a combined heat and power integrated biomass gasificationinternal combustion engine system by using aspen plus. 95:37–44, March 2012. ISSN 03783820. doi: 10.1016/j.fuproc.2011.11.010. URL http://linkinghub.elsevier.com/retrieve/pii/S0378382011003973.

[68] Stephen R Turns. *An Introduction to Combustion: Concepts and Applications*. McGraw Hill, 3 edition, 2012.

[69] Thomas D Johnson, Hannah T Wilner, George V Crawford, Bruce R Johnson, Terry L Krause, Lauren Fillmore, and Steven K Kennedy. CHEApet: a comprehensive energy analysis tool for WWTPs. 2010(13):3416–3445, 2010.

[70] Wayne Doherty, Anthony Reynolds, and David Kennedy. Simulation of a circulating fluidised bed biomass gasifier using ASPEN plus: a performance analysis. 2008. URL http://arrow.dit.ie/engschmeccon/11/.

[71] Naveed Ramzan, Asma Ashraf, Shahid Naveed, and Abdullah Malik. Simulation of hybrid biomass gasification using aspen plus: A comparative performance analysis for food, municipal solid and poultry waste. 35(9):3962–3969, October 2011. ISSN 09619534. doi: 10.1016/j.biombioe.2011.06.005. URL http://linkinghub.elsevier.com/retrieve/pii/S0961953411003291.

[72] P. Arlabosse, S. Chavez, and C. Prevot. Drying of municipal sewage sludge: From a laboratory scale batch indirect dryer to the paddle dryer. 22(2):227–232, 2005.

[73] Philip Wolstenholme and Bo Vestergaard-Hansen. Heat drying biosolids at small to medium size plants: Economics and safety. 2005(2):221–240, 2005.

[74] Jie He, Kristina Gransson, Ulf Sderlind, and Wennan Zhang. Simulation of biomass gasification in a dual fluidized bed gasifier. 2(1):1–10, January 2012. ISSN 2190-6815, 2190-6823. doi: 10.1007/s13399-011-0030-2. URL http://link.springer.com/10.1007/s13399-011-0030-2.

[75] Jiang Qian, Yeong Woo Yoon, Pil Sang Youn, Ji Hye Kim, Don Sun Choi, Jeong-Hoo Choi, Young Chan Choi, and Bongjin Jung. Drying characteristics of sewage sludge. 28(7):1636–1640, June 2011. ISSN 0256-1115, 1975-7220. doi: 10.1007/s11814-011-0009-5. URL http://link.springer.com/10.1007/s11814-011-0009-5.

[76] Maria Puig-Arnavat, Joan Carles Bruno, and Alberto Coronas. Review and analysis of biomass gasification models. 14(9):2841–2851, December 2010. ISSN 13640321. doi: 10.1016/j.rser.2010.07.030. URL http://linkinghub.elsevier.com/retrieve/pii/S1364032110002108.

[77] Ralph Shefflan. *Teach Yourself the Basics of Aspen Plus*. Wiley, 2009.

[78] Giulia Monteleone, Stephen J. McPhail, and Katia Gallucci. Fuel gas clean-up and conditioning. In *Fuel Cells in the Waste-to-Energy Chain*, pages 123–143. Springer London, London, 2012. ISBN 978-1-4471-2368-2, 978-1-4471-2369-9. URL http://www.springerlink.com/index/10.1007/978-1-4471-2369-9_8.

[79] Nimit Nipattummakul, Islam I. Ahmed, Somrat Kerdsuwan, and Ashwani K. Gupta. Hydrogen and syngas production from sewage sludge via steam gasification. 35(21): 11738–11745, November 2010. ISSN 03603199. doi: 10.1016/j.ijhydene.2010.08.032. URL http://linkinghub.elsevier.com/retrieve/pii/S036031991001671X.

[80] Adrian Bejan. *Heat transfer handbook*. J. Wiley, New York, 2003. ISBN 0471390151 9780471390152.

[81] Samsudin Anis and Z.A. Zainal. Tar reduction in biomass producer gas via mechanical, catalytic and thermal methods: A review. 15(5):2355–2377, June 2011. ISSN 13640321. doi: 10.1016/j.rser.2011.02.018. URL http://linkinghub.elsevier.com/retrieve/pii/S1364032111000608.

[82] Yafei Shen and Kunio Yoshikawa. Recent progresses in catalytic tar elimination during biomass gasification or pyrolysisA review. 21:371–392, May 2013. ISSN 13640321. doi: 10.1016/j.rser.2012.12.062. URL http://linkinghub.elsevier.com/retrieve/pii/S136403211300018X.

[83] Stanislaw Szwaja, Viktoria B. Kovacs, Akos Bereczky, and Antal Penninger. Sewage sludge producer gas enriched with methane as a fuel to a spark ignited engine. 2013.

[84] C White, R Steeper, and A Lutz. The hydrogen-fueled internal combustion engine: a technical review. 31(10):1292–1305, August 2006. ISSN 03603199. doi: 10.1016/j.ijhydene.2005.12.001. URL http://linkinghub.elsevier.com/retrieve/pii/S0360319905003721.

[85] Willard W Pulkrabek. *Engineering Fundamentals of the Internal Combustion Engine*. Pearson- Prentice Hall, NJ, 2 edition, 2004.

[86] Monica Rodrigues, Arnaldo Walter, and Andr Faaij. Performance evaluation of atmospheric biomass integrated gasifier combined cycle systems under different strategies for the use of low calorific gases. 48(4):1289–1301, April 2007. ISSN 01968904. doi: 10.1016/j.enconman.2006.09.016. URL http://linkinghub.elsevier.com/retrieve/pii/S0196890406003001.

[87] Firdaus Basrawi, Takanobu Yamada, Kimio Nakanishi, and Soe Naing. Effect of ambient temperature on the performance of micro gas turbine with cogeneration system in cold region. 31(6-7):1058–1067, May 2011. ISSN 13594311. doi: 10.1016/j.applthermaleng.2010.10.033. URL http://linkinghub.elsevier.com/retrieve/pii/S1359431110005144.

[88] Max S. Peters, Klaus D. Timmerhaus, and Ronald E. West. *Plant Design and Economics for Chemical Engineers*. McGraw Hill, New York, 5 edition, 2003.

[89] State and local bonds - bond buyer go 220-bond municipal bond index (WSLB20). Technical report, Federal Reserve Bank of St. Louis, 2013.

[90] Steven Phillips and Timothy J. Eggeman. *Thermochemical ethanol via indirect gasification and mixed alcohol synthesis of lignocellulosic biomass*. Citeseer, 2007. URL http://citeseerx.ist.psu.edu/viewdoc/download?doi=10.1.1.132.4079&rep=rep1&type=pdf.

[91] Eric D. Larson, Haiming Jin, and Fuat E. Celik. Gasification-based fuels and electricity production from biomass, without and with carbon capture and storage. 2005. URL https://www.princeton.edu/pei/energy/publications/texts/LarsonJinCelik-Biofuels-October-2005.pdf.

[92] Electric power monthly. Technical report, Ujnited States Energy Information Administration, June 2013.

[93] United states natural gas industrial price (dollars per thousand cubic feet). Technical Report N3035US3, United States Energy Information Administration, June 2013.

[94] Historical changes of the target federal funds and discount rates. 1971 to present. Technical report, Federal Reserve Bank of New York, 2013.

[95] S. W. Kang, J. I. Dong, J. M. Kim, W. C. Lee, and W. G. Hwang. Gasification and its emission characteristics for dried sewage sludge utilizing a fluidized bed gasifier. 13(3): 180185, 2011. URL http://www.springerlink.com/index/J7357W6766768G45.pdf.

[96] Joan J. Many, Jos L. Snchez, Alberto Gonzalo, and Jess Arauzo. Air gasification of dried sewage sludge in a fluidized bed: effect of the operating conditions and in-bed use of alumina. 19(2):629–636, March 2005. ISSN 0887-0624, 1520-5029. doi: 10.1021/ef0497614. URL http://pubs.acs.org/doi/abs/10.1021/ef0497614.

[97] Tomasz Kupka, Marco Mancini, Michael Irmer, and Roman Weber. Investigation of ash deposit formation during co-firing of coal with sewage sludge, saw-dust and refuse derived fuel. 87(12):2824–2837, September 2008. ISSN 00162361. doi: 10.1016/j.fuel.2008.01.024. URL http://linkinghub.elsevier.com/retrieve/pii/S0016236108000288.

[98] Mehrdokht B. Nikoo and Nader Mahinpey. Simulation of biomass gasification in fluidized bed reactor using ASPEN PLUS. 32(12):1245–1254, December 2008. ISSN 09619534. doi: 10.1016/j.biombioe.2008.02.020. URL http://linkinghub.elsevier.com/retrieve/pii/S0961953408000688.

[99] Biomass for small- scale heat and power. 2004.

[100] R. Dias and J. Balestieri. Energetic and exergetic analysis in a firewood boiler. 12(23): 1524, 2004. URL http://www.unimep.br/phpg/editora/revistaspdf/rct23art02.pdf.

[101] Ian C. Kemp. Reducing dryer energy use by process integration and pinch analysis. 23(9-11):2089–2104, September 2005. ISSN 0737-3937, 1532-2300. doi: 10.1080/07373930500210572. URL http://www.tandfonline.com/doi/abs/10.1080/07373930500210572.

[102] Ulrik Henriksen, Jesper Ahrenfeldt, Torben Kvist Jensen, Benny Gbel, Jens Dall Bentzen, Claus Hindsgaul, and Lasse Holst Srensen. The design, construction and operation of a 75kW two-stage gasifier. 31(10-11):1542–1553, August 2006. ISSN 03605442. doi: 10.1016/j.energy.2005.05.031. URL http://linkinghub.elsevier.com/retrieve/pii/S0360544205001246.

APPENDIX - SUPPLEMENTAL ELECTRONIC FILES

The system model described in Sections 2.1-2.7 and displayed in Figure 2.3 is attached as an ASPEN® Plus version 7.3 flowsheet document named System_Model.apw. The model file is fully functional, and includes the capability to simulate both air and steam blown gasification and either a spark-ignition engine or combustion turbine prime mover. All inline FORTRAN codes are embedded within the file. Calibration variables are set to the values described in Section 3.1. Instructions for selecting a mode of operation (air, steam blown; engine or turbine) can be found under the notes tab of the *Setup* page within the program.